THE EFFECT OF WATER INJECTION
ON THE INDICATOR CARD

ROBERT F. WADSWORTH
NED GARRETT
MAYO M. FITZHUGH, JR.

Library
U. S. Naval Postgraduate School
Monterey, California

[illegible] 135

THE EFFECT OF WATER INJECTION ON THE INDICATOR CARD

by

Lieutenant Commander Robert F. Wadsworth, U.S.N.
Lieutenant Commander Ned Garrett, U.S.N.
Lieutenant Mayo M. FitzHugh, Jr., U.S.N.

Submitted in Partial Fulfillment of
the Requirements for the Degree of
Master of Science
in
Aeronautical Engineering
from the
Massachusetts Institute of Technology
1947

thesis
W2

Cambridge, Massachusetts,
23 May 1947.

Professor Joseph S. Newell,
Secretary of the Faculty,
Massachusetts Institute of Technology,
Cambridge, Massachusetts.

Dear Sir:

A thesis entitled "The Effect of Water Injection on the Indicator Card" is herewith submitted in partial fulfillment of the requirements for the degree of Master of Science in Aeronautical Engineering.

ACKNOWLEDGMENT

The authors wish to express their appreciation of the assistance rendered by Professor C. F. Taylor, Associate Professor A. R. Rogowski, Assistant Professor P. M. Ku, Assistant Professor W. A. Leary, Mr. J. C. Livengood, Mr. C. H. Kano, and Mr. J. L. Fardy.

TABLE OF CONTENTS

	Page
Summary	1
Introduction	2
Description of Apparatus	3
Preliminary Procedure	7
Procedure	10
Presentation of Results	13
Discussion of Results	14
Conclusions	19
Bibliography	21
Appendix I (Sample Calculations)	i - iii
Appendix II (Equivalent Cycle)	iv - vi
Tables I and II (Calibrations)	vii - viii
Data Sheet	
Figures and Charts	

LIST OF FIGURES

Fig.

1 Engine Layout.

2 Timing Diagram.

3 Manifold Diagram.

4 Indicator Diagram.

5 Dynamometer Wiring Diagram.

6 Ignition System.

7 Fuel System.

8 Fuel Calibration.

9 Water Calibration.

10 $dP/d\theta$ Cards 45" Hg.

11 $dP/d\theta$ Cards 31" Hg.

12 $dP/d\theta$ Cards 20" Hg.

13 $dP/d\theta$ Cards 31" Hg., Best Power Spark Advance (BPSA).

14 Pressure-Volume Cards, 45" Hg.

15 Pressure-Volume Cards, 31" Hg.

16 Pressure-Volume Cards, 20" Hg.

17 Pressure-Volume Cards, 31" Hg. (BPSA).

18 Plot of IMEP vs W/F.

19 Plot of Eff. vs W/F.

20 Plot of e vs W/F.

21 Plot of e, IMEP, and Eff. vs W/F (31" Hg. BPSA).

22 Plot of S.A. vs W/F (31" Hg. BPSA).

23 Plot of $dP/d\theta$ vs W/F (all runs).

24 Photo of Sample Indicator Card without water injection.

25 Photo of Sample Indicator Card with water injection.

26 Photo of Manifold and Cylinder.

SUMMARY

This investigation was made to determine the effects of manifold water injection on the indicator diagrams and from these diagrams to calculate engine performance.

In carrying out this study, four runs were made. The first three were made at inlet pressures of 31", 20" and 45" of mercury and with a constant spark advance set for best power with no water injected, all other conditions being held constant. From these runs it was determined that the indicated mean effective pressure and the volumetric efficiency decreased with an increase in water rate, while the indicated efficiency remained substantially constant up to the point where the engine commenced to miss. With an increase in inlet pressure it was possible to inject more water before the engine misfired.

The fourth run was made at an inlet pressure of 31" of mercury but with the spark set at best power for each water rate used. From this run it was found that because of partial elimination of time losses, the indicated mean effective pressure decreased with an increase in water rate but not as much as in previous runs, while the indicated efficiency showed a slight increase. The volumetric efficiency dropped the same as in the previous run because the inlet conditions were not changed.

INTRODUCTION

The demand for higher engine outputs, greater than those allowable from detonation limited engines, has led to much investigation of the effect of water injection on detonation suppression and on overall engine performance. Most of these investigations have centered on the effect of water on detonation, and on the allowable increase in power which can be drawn from the engine after the suppression of detonation.

The purpose of this investigation has been to examine the effect of manifold water injection on the indicator card, and by use of data obtained from the indicator card to evaluate the indicated performance of the internal combustion engine. While much published data on water injection effects are available, very few experiments relating the effects of water injection to the indicator card have been conducted.

This study was conducted in the Sloan Automotive Laboratory at Massachusetts Institute of Technology by Lieut. Comdr. R. F. Wadsworth, U.S.N., Lieut. Comdr. N. Garrett, U.S.N., and Lieut. M. M. FitzHugh, U.S.N. Professor W. A. Leary, of the M.I.T. staff, was supervisor.

DESCRIPTION OF APPARATUS

The test equipment included: A Coordinating Fuel Research (CFR) engine delivering power to a dynamometer; a high speed MIT engine indicator and MIT diagram converter; an American Bosch fuel injector pump for water injection; and instruments for measuring air, fuel, water and engine speed. Fuel was vaporized in a heated vaporization tank; water was injected by a Bendix injection nozzle into the intake manifold. A schematic diagram of the engine set-up is shown in Fig. 1.

Engine

A standard 4-cycle one-cylinder CFR engine No. 469373 made by Waukesha Motor Co. was used. The bore was 3.25 in. in diameter, the stroke 4.50 in. and the displacement 37.33 cubic in. The compression ratio could be varied from 4 to 10 but was set for 6.63 for this investigation. The standard CFR engine is fully described in the CFR Handbook, 1944 edition (reference 1).

Dynamometer

A 5-hp motor-generator set made by the Star Electric Motor Co. was used as a motor to turn over the CFR engine for starting and motoring and as a generator to absorb the power delivered while the engine was firing.

MIT Indicator

The high speed indicator is shown schematically in Figs. 4 and 5. A description of this instrument is included in references 2 and 8.

Converter

The diagram converter was merely a linkage device to convert the pressure versus crank angle diagram of high speed indicator to a pressure versus volume diagram.

Water Injection

The American Bosch fuel injection pump was used to inject water and was mounted on the half time shaft of the engine. Distilled water flowed by gravity from a two gallon tank into a water rotometer and then into the suction side of the pump. The pump also had a built-in surge tank and a centrifugal booster pump which gave a very smooth flow reading. A lock screw adjustment was used to give very fine control of water rate. A Standard Bendix (No. 135026, Serial 42) fuel injection nozzle was used for water injection into the manifold. The nozzle was set to open at 500 lbs. per sq. in. at which a fine spray in a 45 degree cone was attained.

Fuel System

The gasoline used in this experiment was standard 100 octane leaded aviation gasoline. This gasoline was taken from the mains of the Sloan lab-

oratory and passed through a fuel pump into a bubble separation tank, through the fuel rotometer and into the heated vaporizing tank. By a combination of two needle valves between the vaporizing tank and fuel rotometer accurate control of fuel flow was assured. A schematic diagram of the fuel system is shown in Fig. 7.

Detonation Detection

Detonation was detected by a Draper detonation pickup and a Dumont oscillograph No. 722. This equipment was only used to test for detonation at high manifold pressures. Most of the runs in this investigation were made below the incipient detonation level.

Air System

Air to the vaporizing tank was taken either from the laboratory high pressure main or from the test room at atmospheric pressure. A Worthington air compressor, driven by a 75 hp Wagner Electric Motor, supplied the high pressure air. When the air was drawn from the high pressure main, it was led to a regulator and a regulator valve through a .515 inch calibrated orifice into a surge tank through a throttle valve, a check valve, and into the vaporizing tank as shown in Fig. 1.

Speed Control

Speed control was measured with a tachometer supplemented by a strobotac for finer adjustments. A drop wire rheostat in the shunt field of the dynamometer was employed for speed control.

Ignition

The ignition wiring diagram is shown in Fig. 6.

PRELIMINARY PROCEDURE

Prior to commencement of this experiment, it was necessary to spend considerable time in testing and connecting up the apparatus as shown in Fig. 1. In order to simulate aircraft sea level operating conditions, it was decided to use 100 octane fuel, a fixed compression ratio, and water injection into the manifold.

A special manifold was designed, as shown in Fig. 3. The nozzle was aimed as close as practicable toward the inlet valve. Two thermometers were placed in this manifold. One was mounted before the nozzle, and one between the nozzle, and the inlet valve. The thermometer located after the nozzle was shielded to keep the water spray off the mercury bulb.

It was also necessary to calibrate the fuel and water rotometers for at least two different room temperatures 10 degrees apart so that interpolations could be made in between the curves at various temperatures. The method of calibration in every case consisted essentially of weighing the amount of liquid which passed through the rotometer in a measured interval of time, during which the rotometer setting was maintained at a constant level. Calibration curves were made from the data of tables I and II and plotted in Figs. 8 and 9. After completion of the final runs, the water rotometer was recalibrated with the engine

running at normal operating temperatures so that all water readings taken during the runs were within one degree of the calibrated temperature.

The air induction system was tested for leaks at 48 inches of mercury and checked until there was less than .4 inches per minute pressure drop. Computations showed this leakage to be well below one percent of the air used by the engine.

At first, it was thought that water injection timing would have little effect because it was injected into the manifold. The inlet valve opened at 14 degrees after top center and closed 234 degrees after top center. For the runs for which data is presented, the injector nozzle started injection at 36 degrees after top center and completed injection 79 degrees after top center for the high water rates. This allowed 155 degrees for the water to mix with the charge and to insure that all the water would be taken into the cylinder on each stroke. Several runs were made with the injection timed 360 degrees from this, that is, allowing the water to accumulate in the manifold near the intake valve while the intake was closed. Little or no differences were noted in the indicator card for the two timing conditions. A valve timing diagram is shown in Figure 2.

Due to the shape of the shrouded inlet valve, the spark plug was shifted on the opposite side of the cylinder from the normal position to prevent the water from

grounding out the plug. Runs were made, however, in both positions and practically no differences were observed in the indicator card for equal water rates. The engine stopped running at lower water rates in every case when the spark plug and shrouded inlet valve were placed in the designed operating condition.

PROCEDURE

The following set of conditions was adopted as standard:

Inlet temperature - 160 degrees F (read at vaporizing tank before water injection nozzle)
Oil temperature - 150 degrees F
Jacket temperature - 212 degrees F
Engine speed - 1200 rpm
Fuel-air ratio - .0782
Compression ratio - 6.63
Exhaust pressure - 32" Hg.
Spark advance - Three sets of runs were made with best power spark advance set without water injection for each inlet pressure of 45", 31" and 20" Hg. One run was made with a variable spark advance, best power being set for each water/fuel ratio used for inlet pressure of 31" Hg.

A warm-up period of one and one-half hours was required as a daily routine prior to making recorded runs. At least twenty minutes were allowed to elapse between points for steady conditions. The engine was brought as near as possible to the standard temperatures by using steam to heat the oil tank and inlet air before starting. An electric air heater was used for finer control of inlet temperatures when necessary.

After steady operating conditions were attained, an indicator card was taken without water injection while all conditions were held constant. This was repeated for several water rates up to the point where the engine began to miss. These runs were made at inlet pressures of 45", 31" and 20" of mercury, the spark advance in each case being set for best power with no water and then being held constant for the remainder of the run. At 45" of mercury inlet pressure heavy detonation was encountered. After the first indicator card was taken with no water, the water rate was increased until only incipient detonation occurred. The remainder of this run was made in the same manner as the 31" and 20" of mercury inlet pressure runs.

After completion of the above runs, an additional run was made under the same conditions as the run made with an inlet pressure of 31" of mercury, except that the spark advance was adjusted to best power for each new water rate. It was found that the best power setting could be approximated by measuring the difference in degrees after top center between the pressure peaks of the indicator cards taken with no water and cards taken at successive water rates for the preceding run made at constant spark advance and at 31" of mercury inlet pressure. Finer adjustment was then made by noting with the strobotac any effect of small spark timing adjustment on the engine speed. It was found that in each case of varying water rate, the

best power spark advance occurred at a point which caused all the indicator cards of this run to peak at approximately the same number of degrees after top center as shown in Fig. 13.

PRESENTATION OF RESULTS

Results are presented in the form of diagrams and performance curves as follows:

Figures 10, 11, 12, and 13: Pressure versus crank-angle diagrams. Cards taken with the same inlet pressures are superimposed upon each other. The diagrams were traced directly from the cards obtained from the MIT High Speed Indicator. They show the effect of water injection into the intake manifold.

Figures 14, 15, 16, and 17: Pressure-volume diagrams presented in the same way as above. These diagrams were converted from the pressure versus crank-angle cards. This operation was perhaps the largest source of error.

Figure 18: Indicated mean effective pressure versus water/fuel ratio for different inlet pressures.

Figure 19: Indicated efficiency versus water/fuel ratio for different inlet pressures.

Figure 20: Volumetric efficiency versus water/fuel ratio for different inlet pressures.

Figure 21: Indicated mean effective pressure, efficiency, and volumetric efficiency versus water/fuel ratio for 31" of mercury inlet pressure with constant spark advance and with best power spark advance. These curves show the effect of partial elimination of time losses in the process.

Figure 22: Best power spark advance versus water/fuel ratio.

Figure 23: Rate of pressure rise versus water/fuel ratio for different inlet pressures.

DISCUSSION OF RESULTS

Effect on Area of P-V Diagrams and Indicated Efficiency

Fig. 19 shows that the indicated efficiency remains very nearly constant for increasing water/fuel ratio without change in spark advance. However, the area under the pressure-volume diagram (Fig. 14, 15, 16, 17) which was used to compute the indicated mean effective pressure (Fig. 18) and efficiency (Fig. 19) apparently shows a marked decrease in magnitude as the water/fuel ratio increases. This apparent decrease is caused by the greatly reduced flame speed and a large area loss generally associated with time loss. It will be noted, however, that there is a considerable increase in area on the expansion stroke. It is this compensating area which keeps the efficiency constant, or nearly so. As the water/fuel rate increases, the time loss area increases, but there is a corresponding increase in the area under the expansion curve.

Part of the increase in area may be accounted for in the following manner (Appendix II). Suppose that a normal Fuel-Air cycle is considered. For any point on the expansion line there will be found a certain pressure. Consider now that another process is carried out in which the compression stroke is identically the same as before. Now, instead of burning at constant volume, let the burning take place at a changing volume. By constructing a pressure-volume diagram for a standard fuel-air cycle, the area under

the new burning line may be computed and the new internal energy of the gases in the cylinder may be found. It will be found that since the gases have done less work up to the new point, the pressure and the temperature at the same volume point will be higher than the pressure and temperature on the original pressure-volume diagram. Expanding from this point isentropically gives a higher expansion curve, and therefore some additional area, which compensates in part for the time loss involved in the constant volume burning.

The rest of the increase in the compensating area is due entirely to the effect of the addition of water to the charge. The mean cylinder temperatures are lower throughout the cycle and the dissociation of the charge, including the water, is decreased with the temperature decrease (R. Wiebe, 4). This leads to a higher percentage of CO_2 and H_2O in the products of combustion, and an increased amount of heat obtained from the fuel. The same author has constructed theoretical fuel-air-water charts and shows an increase in efficiency with water/fuel rate. This agrees well with the results of this investigation, since it was found that with spark advance adjusted to eliminate the time losses as much as possible, the actual indicated efficiency increased (Fig. 21). The theoretical increase in efficiency was greater, since the time losses were not entirely eliminated in the actual engine process.

Kuhring (6), in a test of a Jaguar aircraft engine, noted a decrease in cylinder temperature when water is added. A decrease in heat transfer to the cooling water was noted in the present investigation, but the cooling water temperatures were held constant by varying the rate of coolant flow.

Effect on Volumetric Efficiency

The volumetric efficiency (Figs. 20 and 21) dropped off with an increase in water rate because the water was injected into the manifold, and the water and water vapor displaced some of the air which would have entered the cylinder. For this investigation the inlet conditions used in calculating the volumetric efficiency are defined by the pressure and temperature of the air and fuel vapor in the mixing tank.

Effect on Indicated Mean Effective Pressure

The indicated mean effective pressure (Figs. 18 and 21) dropped with increasing water/fuel ratios mainly because the volumetric efficiency was reduced. The expression stating that IMEP varies directly with $e\rho_i(FE_c\eta_i)$ shows that if inlet conditions are kept constant, the fuel-air ratio remains constant, the same fuel is used, and, as in this case, the indicated efficiency remains substantially constant, then the indicated mean effective pressure is proportional to volumetric efficiency and should be expected to decrease.

On the other hand, had the water been injected into the cylinder after the valves were closed, there would be no change in volumetric efficiency and the indicated mean effective pressure would increase, as has been shown by several other investigations (10).

Effect on Compression Stroke

The bulge in the compression line (Figs. 10, 11 and 12) at high water rates is very likely caused by liquid water impinging on the hot cylinder surfaces and transferring heat from them. This water flashes to steam, and the heat added to the charge increases the sensible energy of the system and causes a pressure rise in the cylinder. At the lower water rates it is likely that not enough liquid water gets into the cylinder to cause a noticeable change in the compression process. Ordinarily, it would be expected that when water is introduced to a heated charge, the effect would be to lower the pressure and the temperature, and a thermometer placed on the intake manifold between the injection nozzle and the inlet valve showed such a decrease in the temperature of the charge. However, in the case of extreme water rates, there is actually enough heat transferred from the cylinder walls to increase the cylinder pressure.

Effect on Spark Advance

It is to be expected that with constant piston speed and constant inlet conditions, the flame speed will decrease

with an inert diluent in the charge. The results show that the rate of pressure rise (Fig. 23) is nearly linear with water/fuel ratio. Also, the spark advance must be increased as the flame speed decreases to keep the time losses at a minimum. The results show that the spark advance (Fig. 22) required for best power is also a linear function of the water/fuel ratio.

Experimental Error

In this work it was found that the greatest source of error was in the transfer of the dp/dθ diagram to the pressure-volume diagram. The utmost care in the operation of the MIT transfer machine is required.

After the data for this investigation had been obtained, test runs were made under the same conditions as previous runs and the computations from these runs produced results within one and one-half percent of the original runs.

CONCLUSIONS

As a result of this investigation of the effects of manifold water injection on the engine indicator card, the following conclusions may be drawn:

1. The indicated efficiency remains substantially constant within the range of water/fuel ratios needed to quell detonation when the spark is set for best power with no injection. However, adjusting the spark for best power at each water rate causes the efficiency to increase within the same range.
2. As the water/fuel ratio is increased, the volumetric efficiency decreases linearly. This decrease is the same for engine operation under constant best power spark advance set for no water rate and for best power spark advance set for each water rate, since the inlet conditions do not change.
3. The indicated mean effective pressure decreases with an increase in water/fuel ratio, the decrease being less when best power spark is set for each water rate than when constant spark advance is used.
4. The maximum pressures of the cycle decrease with water/fuel ratio increase, the decrease being greater in the case of constant spark advance set for best power with no water. The pressure peaks also occur further after top center with water rate increase except for best power spark advance, where they all peak at approximately the same distance after top center.

5. The time losses increase with water rate, but the expansion line becomes higher, partially compensating for the time loss.
6. The best power spark advance varies linearly with water/fuel ratio, increasing with an increase in the water rate.
7. The amount of water that can be injected into the manifold of an engine before it commences to miss is a function of the inlet pressure. An engine with higher inlet pressure is able to absorb a greater amount of water before missing.

REFERENCES

1. THE CFR HANDBOOK, 1944 Edition.
2. TAYLOR, E. S. and DRAPER, C. S., "A NEW HIGH-SPEED ENGINE INDICATOR", Mechanical Engineering, March 1933.
3. TAYLOR, C. F. and TAYLOR, E. S., "THE INTERNAL COMBUSTION ENGINE", International Textbook Company, 1938.
4. WIEBE, R., SCHULTZ, J. F., PORTER, J. C., "MOLLIER DIAGRAMS FOR THEORETICAL ALCOHOL-AIR AND OCTANE-WATER-AIR MIXTURES", Industrial and Engineering Chemistry, May 1942.
5. WIEBE, R., SHULTZ, J. F., PORTER, J. C., Industrial and Engineering Chemistry, Volume 36, Number 7, July 1946.
6. KUHRING, M. S., Canadian Journal of Research, 16A 149, 1938.
7. HOTTEL, H. C., EBERHARDT, J. E., "A MOLLIER DIAGRAM FOR THE INTERNAL COMBUSTION ENGINE", Chemical Reviews, Volume 21, Number 3, December 1937.
8. HELDT, P. M., "THE M.I.T. INDICATOR", Automotive Industries, July 28, 1944.
9. "SUPPLEMENTARY INJECTION OF WATER AND WATER-ALCOHOL MIXTURES", Air Corps, Materiel Division Report, November 5, 1941.
10. SEIBELS, R. E., WASHINGTON, T., MACLACHLAN, J. R., "AN INVESTIGATION OF THE EFFECT OF DIRECT WATER INJECTION ON DETONATION", Thesis, M.I.T. Library, 1946.
11. KEENAN, J., "THERMODYNAMICS", John Wiley & Sons, Inc., 1941.

APPENDIX I

Symbols Used in Sample Calculations

A - Area of indicator card in square inches.

e - Volumetric efficiency.

E_c - Heating value of fuel (19000 Btu per lb).

E_{comb} - Energy due to the change in base of the fuel-air mixture.

E_s - Sensible energy of the mixture.

f - Ratio of residual gas to gas in total charge.

F/A - Fuel-Air Ratio.

h - Inches of water pressure difference across the orifice.

h_s - Sensible enthalpy of the mixture.

IHP - Indicated horse power.

IMEP - Indicated mean effective pressure.

K - Spring constant of indicator lbs/in.

L - Length of indicator card (5 inches).

M_a - Lbs of air/sec. supplied.

M_f - Lbs of fuel/sec. supplied.

n - Number of suction strokes/sec.

N - RPM = 1200.

η_I - Indicated thermal efficiency

P - Pressure before orifice in inches of Hg.

P_i - Inlet pressure in lbs/in^2 measured in the mixing tank.

ρ_i - Density at inlet lbs/ft^3.

R - 53.3 ft lbs/lb ^{o}R.

T - Temperature at orifice °R.

T_1 - Inlet temperature of air.

2545 - Conversion factor (Btu/IHP-hr).

.01825 - Conversion factor and orifice coefficient for .515 inch diameter orifice.

SAMPLE CALCULATIONS

For run with 20" of mercury inlet pressure:

$$M_a = .01825\sqrt{\frac{P}{T}h} = .01825\sqrt{\frac{29.74 \times 2.75}{538}} = .00712 \text{ lbs. air/sec.}$$

$$F/A = \frac{M_f}{M_a}$$

$$M_f = F/A \times M_a = .0782 \times .00712 = .000556 \text{ lbs. fuel/sec.}$$

$$IHP = \frac{IMEP \times V_d \times N}{2 \times 12 \times 33000}$$

$$IMEP = \frac{A \times K}{L} = \frac{3.542 \times 100}{5}$$

$$IHP = \frac{70.85 \times 37.33 \times 1200}{2 \times 12 \times 33000} = 4.0 \text{ H.P.}$$

$$\eta_I = \frac{IHP \times 2545}{M_f \times E_c \times 3600} = \frac{IHP \times .0000372}{M_f} = \frac{4.0 \times .0000372}{.000556} = .278$$

$$e = \frac{M_a}{\rho_i \; n \; V_d}$$

$$\rho_i = \frac{P_i}{R\,T_i} \qquad 20\text{" Hg.} = 9.82 \text{ lbs/in.}$$

$$\rho_i = \frac{9.82 \times 144}{53.345 \times 620} = .0428 \text{ lbs/cubic foot.}$$

$$e = \frac{.00712 \times 1728}{.0428 \times 37.33 \times 10} = .77$$

APPENDIX II

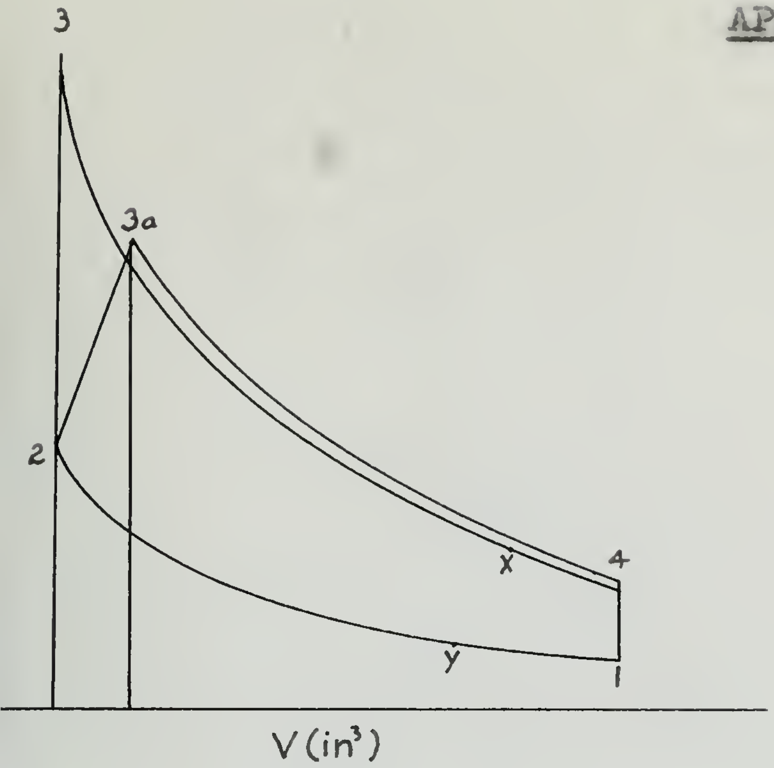

Data from P.-V. diagram

V_D = 37.33 cu. in.

V_{CL} = 6.628 cu. in.

p_x = 71.2 lbs/in.^{2}

V_x = 36.88 cu. in.

p_y = 22.2 lbs/in.^{2}

V_y = 32.93 cu. in.

Construct the equivalent cycle for 31" Hg.

B = Mass air/cycle = .00118 lbs. air/cycle

$v_{chart\ x} = v_{cyl} \times \frac{1-f}{B}$

$f = \frac{V_2}{V_1}$

By trial and error find f = .052

Using this f find:

$v_{chart\ x}$ = 17.15 cu. ft.

$v_{chart\ 2}$ = 3.08 " "

$v_{chart\ y}$ = 15.33 " "

$v_{chart\ 1}$ = 20.45 " "

At state 1:

$T = 800$ $E_s = 57$ $H_s = 114$ $p = 150$ $v = 20.45$

Compress isentropically to $v = 3.08$ (state 2)

At state 2:

$T = 1370$ $E_s = 193$ $H_s = 290$ $p = 164$ $v = 3.08$

Burn at constant volume:

$E_{comb.} = 1507(1-f) + 300 f = 1443$

At state 3:

$T = 5100$ $E = 1636$ $p = 705$ $v = 3.08$

Expand isentropically to $v = 20.45$ cu. in.

At state 4:

$p_4 = 68$ lbs/in^2 $v = 20.45$ $E = 1025$

From this data compute engine performance.

First Law of Thermodynamics $E_4 - E_1 = Q - W$

$W = E_1 - E_4 = 475$ Btu/lb.

IMEP = work/cycle = 148 lb/in.^{2}

η_i = IMEP/(1-f) F E_c = 33.7%

Now assume that the charge burns at varying volume. Find from actual engine data the volume at which peak pressure occurs is 8.86 cu. in. This gives a v_{chart} = 4.13 cu. ft.

By trial and error find end pressure at this volume = 520 lbs./sq. in., and work done in this process = 64 Btu.

Expanding from this point isentropically, find that

P_4 = 70 lbs./in.^{2} , E_4 = 1065

$$E_1 - E_4 = 1500-1065 = 435$$

$$= 30.85$$

If we assume cylinder pressure ended on original expansion line, and subtract the work lost, the efficiency = 30.2%.

TABLE I

Fuel Rotometer Calibration

3/13/47 $T_{fuel} = 78^{\circ}F$

Rotometer Readings	Time Secs.	Wt. gms.	lbs/sec
5.4	133.3	10	.000165
7.0	53.6	10	.000411
7.75	44.3	10	.00498
8.625	71.6	20	.000615
8.92	65.6	20	.000671
9.65	58.2	20	.000758
10.3	51.8	20	.00085
11.05	45.44	20	.00097
11.95	61.00	30	.001085
12.35	57.50	30	.00115
13.6	49.7	30	.001328
14.9	43.1	30	.001535
11.6	43.45	20	.001015
13.02	36.15	20	.00122
15.8	40.2	30	.001645
15.81	52.0	40	.001692
16.88	47.9	40	.001840

Fuel Rotometer Calibration

2/11/47 $T_{fuel} = 68^{\circ}F$

Rotometer Readings	Time Secs.	Wt. gms.	lbs/sec
5.20	82.7	5	.0001333
6.37	85.45	10	.000256
7.8	91.9	20	.000481
8.7	73.9	20	.0005975
9.6	61.45	20	.000718
10.2	27.1	10	.000813
10.9	48.6	20	.000906
11.55	44.4	20	.000994
12.20	82.24	40	.001072
12.60	77.4	40	.00114
13.22	71.1	40	.00124
14.05	64.4	40	.001371
14.88	59.8	40	.001475
15.71	54.37	40	.001625
16.72	49.36	40	.001791
17.80	44.95	40	.001967
18.40	43.00	40	.002050
18.2	44.4	40	.001988
18.75	41.88	40	.00210
18.60	42.4	40	.002085
19.66	38.1	40	.002315
20.75	34.54	40	.002555
17.4	45.7	40	.001927
17.1	47.8	40	.001845
14.83	59.85	40	.001475

TABLE II

Water Rotometer Calibration

4/17/47 $T_{water} = 80^\circ F$

(Engine Running at operating temperatures)

Rotometer Reading	Time Secs.	Wt. gms.	lbs/sec
11	628.0	20	.0000701
23	308.3	20	.0001428
35	154.7	20	.000285
15.5	535.7	20	.0000823
31	198.8	20	.000221
41	118.0	20	.000373
50	113.25	30	.000583
58	102.2	40	.000862
63.80	105.2	50	.00134
60.5	113.1	50	.000973
72.0	111.3	70	.001385
77.7	97.95	70	.001575
83.0	84.57	70	.00182
88.0	75.9	70	.00203
99.7	69.7	80	.00253
65.5	99.8	50	.001104
53.2	126.88	40	.000695
48.1	134.82	30	.000491
16.5	568.0	20	.0000775
20	348.4	20	.00001265

M.I.T. AERO ENGINE LABORATORY

ENGINE CFR

BORE 3.25" STROKE 4.5" COMPRESSION RATIO 6.63

REMARKS	DATE	TIME	RUN	RPM	B.L	OIL TEMP	JAC TEMP	OIL PRESS	BAR. (CORR)	P_i	P_e	T_i	AIR CONS.	FUEL CONS.	$\frac{F}{A}$	S.A.	ΔP_e	ΔP_i	$T_{ORIF.}$	ΔP_{ORIF}	$\Delta P_{ABS. ORIF.}$	FUEL PRESS	T_{i_2}	T_{FUEL}	T_{WATER}	FUEL ROTO	WATER ROTO
	4/12/47								"HG	"HG	"HG	°F	LBS/SEC	LBS/SEC			"HG	"HG	°F	"H₂O	"HG	LBS/IN²	°F	°F	°F		
	"	1130	1	1200	22.1	150	210	44	29.95	31	32	160	.01180	.000923	.0782	19	2.05	1.05	77	6.8	3.1	20	170	80	80	10.74	0
	"	1210	2	"	22.0	"	"	"	"	"	"	"	.01170	.000916	"	"	"	"	79	6.7	3.05	19	132	81	80	10.70	28
	"	1237	3	"	21.8	"	209	43	"	"	"	"	.01160	.000907	"	"	"	"	80	6.6	3.30	"	124	81	81	10.6	51
	"	1256	4	"	21.2	"	"	"	"	"	"	"	.01142	.000894	"	"	"	"	81	6.4	3.1	"	116	83	81	10.54	67
ENGINE MISSING →	"	1317	5	"	19.2	"	"	41	"	"	"	"	.01131	.000885	"	"	"	"	81	6.25	3.3	"	111	83	81	10.37	79
DETONATING. →	4/15/47	1100	1	1200	17.5	150	211	40	30.00	45	32	160	.0177	.001385	.0782	17	2.0	15.0	79.5	10.7	17.5	20	170	82	79	13.85	0
INCIPIENT DETONATION →	"	1125	2	"	17.5	"	210	"	"	"	"	"	.0176	.001375	"	"	"	"	80	10.55	17.6	"	146	85	79	13.75	23
	"	1150	3	"	17.5	"	"	"	"	"	"	"	.0176	.001375	"	"	"	"	80	10.55	17.6	"	134	85	79	13.70	36
	"	1230	4	"	15.7	"	"	33	"	"	"	"	.0172	.001345	"	"	"	"	81	10.1	17.65	"	119	85	80	13.50	96
	"	1315	5	"	17.0	"	"	33	"	"	"	"	.01745	.001365	"	"	"	"	81	10.35	17.85	"	122	86	80	13.6	66
	"	1515	6	"	16.9	"	"	39	"	"	"	"	.01733	.001355	"	"	"	"	80	10.15	18.0	19	116	86	80	13.5	79
	4/17/47	1030	1	1200	11.3	150	209	46	29.74	20	32	160	.00727	.000569	.0782	21	2.26	9.74	76	2.85	0	20	173	80	78	8.15	0
	"	1110	2	"	11.1	"	"	"	"	"	"	"	.00712	.000556	"	"	"	"	78	2.76	0	"	122	81	78	8.02	26
	"	1140	3	"	10.7	"	"	"	"	"	"	"	.00705	.000551	"	"	"	"	79	2.70	0	"	116	81	78	8.0	40
	"	1200	4	"		"	"	"	"	"	"	"	.00692	.000541	"	"	"	"	78	2.6	0	"	110	80	78	7.9	49
	"	1225	5	"	10.2	"	"	"	"	"	"	"	.00707	.000553	"	"	"	"	80	2.72	0	"	117	81	78	8.0	35
	"																										
	4/29/47	1027	1	1200	22.7	150	211	42	30.20	31	32	160	.01175	.00092	.0782	19	1.80	.80	76	5.82	8.02	20	172	80	80	10.72	0
	"	1052	2	"	22.3	"	210	"	"	"	"	"	.01168	.000912	"	20.3	"	"	76	5.72	8.18	"	129	80	80	10.68	29
PEAK TOO FAR RIGHT	"	1100	3a	"	21.7	"	"	"	"	"	"	"	.01147	.000896	"	22.2	"	"	"	5.50	8.22	"	117	80	80	10.52	53.5
PEAK O.K.	"	1125	3	"	21.7	"	"	"	"	"	"	"	.01147	.000896	"	25.0	"	"	"	5.80	8.22	"	116	80	80	10.52	54.5
PEAK TOO FAR LEFT	"	1200	4a	"	21.1	"	"	"	"	"	"	"	.01132	.000887	"	30.0	"	"	77	5.38	8.15	"	108	80	80	10.48	68.5
PEAK O.K.	"	1207	4	"	21.3	"	"	"	"	"	"	"	.01132	.000887	"	28.5	"	"	"	5.38	8.15	"	111	81	80	10.48	69.0
MISSING 5 TIMES PER MINUTE	"	1235	5	"	21.2	"	"	"	"	"	"	"	.01120	.000876	"	30.0	"	"	"	5.28	8.15	"	106	81	80	10.38	74.0
CHECK POINT FOR REPRODUCABILITY	"	1315	6	"	22.0	"	"	"	"	"	"	"	.01153	.000902	"	19	"	"	"	5.61	8.05	"	114	81	80	10.57	54.0

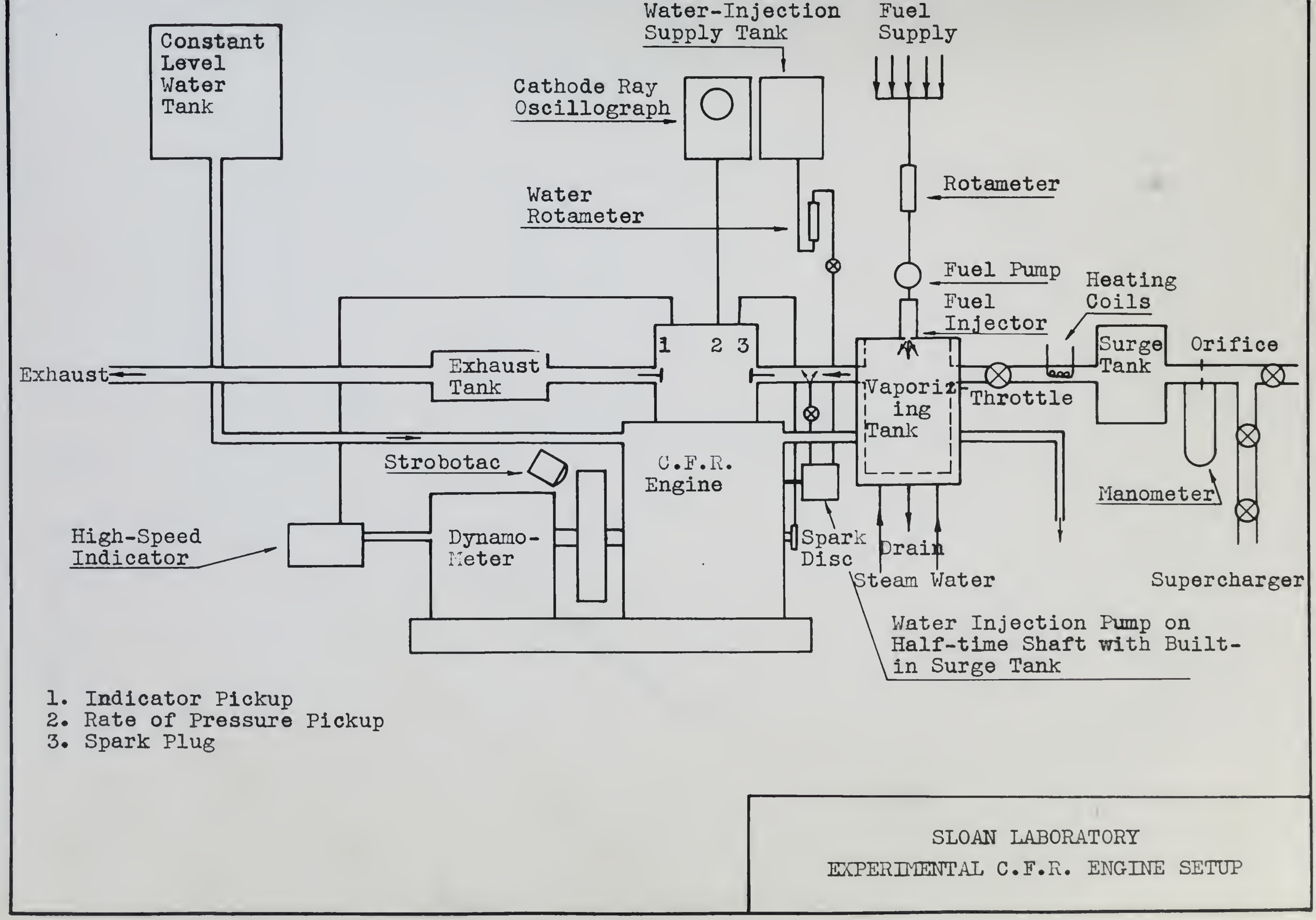
Constant Level Water Tank
Water-Injection Supply Tank
Fuel Supply
Cathode Ray Oscillograph
Water Rotameter
Rotameter
Fuel Pump
Fuel Injector
Heating Coils
Surge Tank
Orifice
Exhaust
Exhaust Tank
1
2
3
Vaporizing Tank
Throttle
Strobotac
C.F.R. Engine
Manometer
High-Speed Indicator
Dynamo-Meter
Spark Disc
Drain
Steam Water
Supercharger
Water Injection Pump on Half-time Shaft with Built-in Surge Tank
1. Indicator Pickup
2. Rate of Pressure Pickup
3. Spark Plug
SLOAN LABORATORY
EXPERIMENTAL C.F.R. ENGINE SETUP

Fig. 1

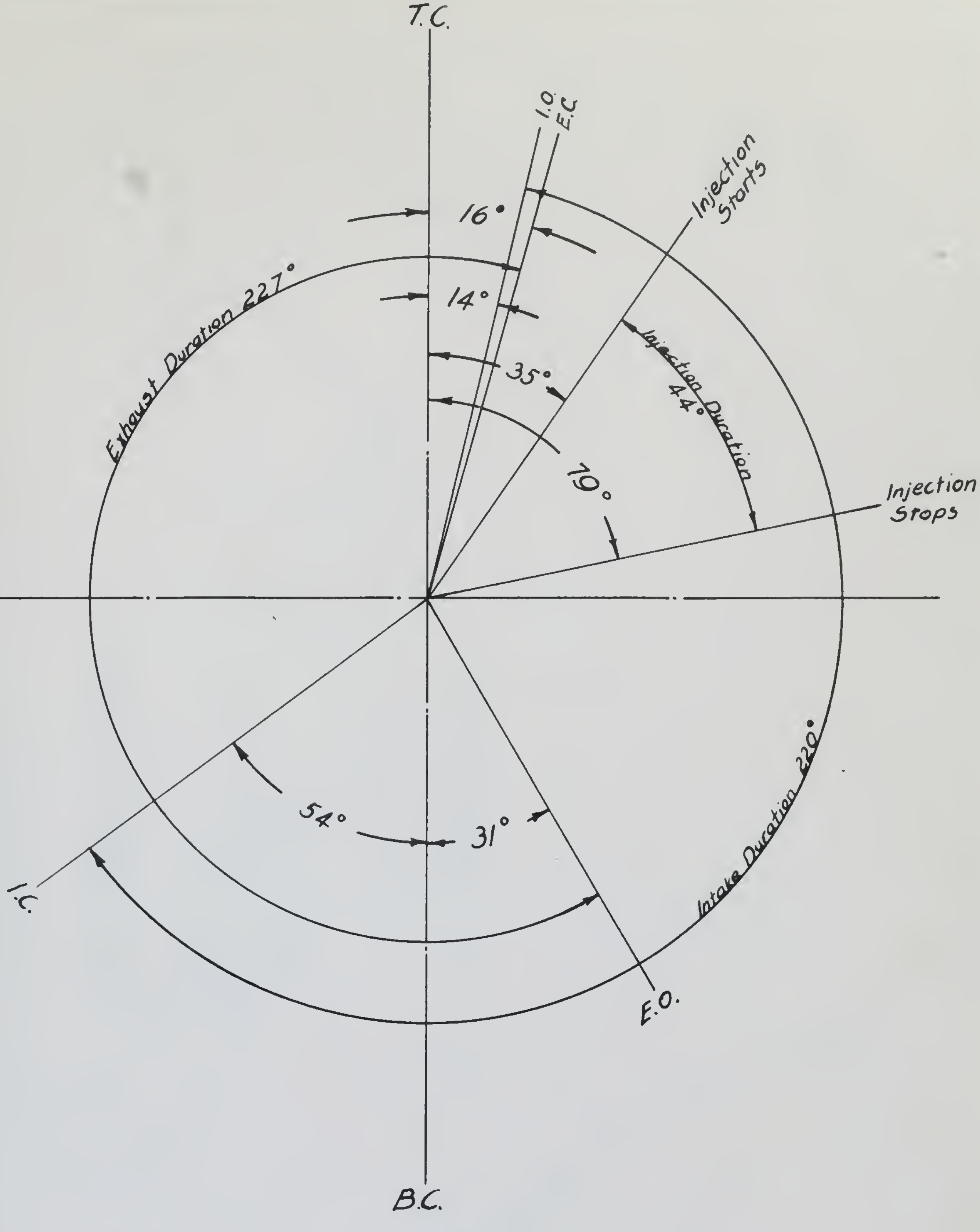

Timing Diagram

Fig. 2

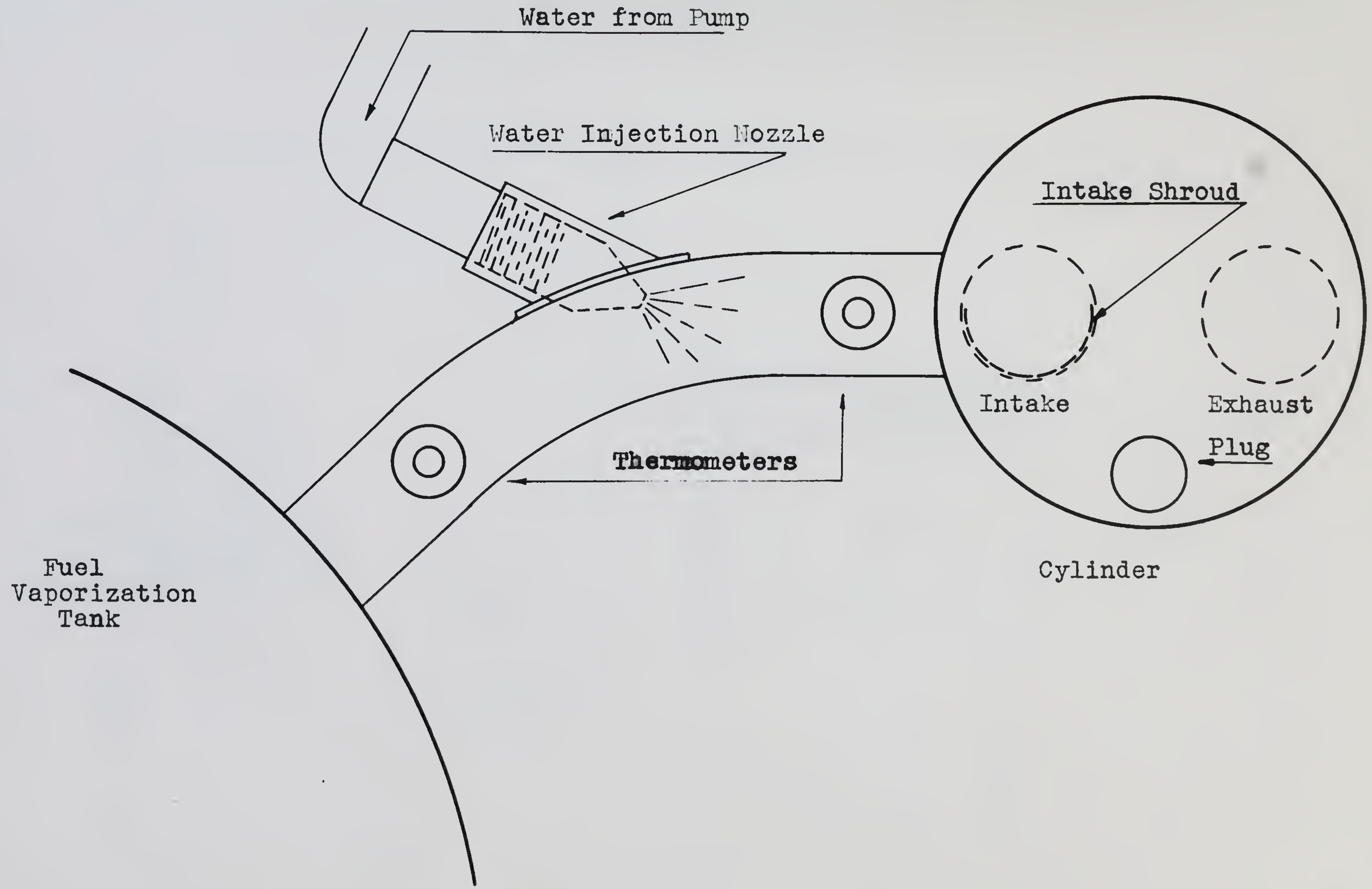

DIAGRAMATIC DRAWING OF SYSTEM USED
TO INJECT WATER INTO MANIFOLD

Fig.3

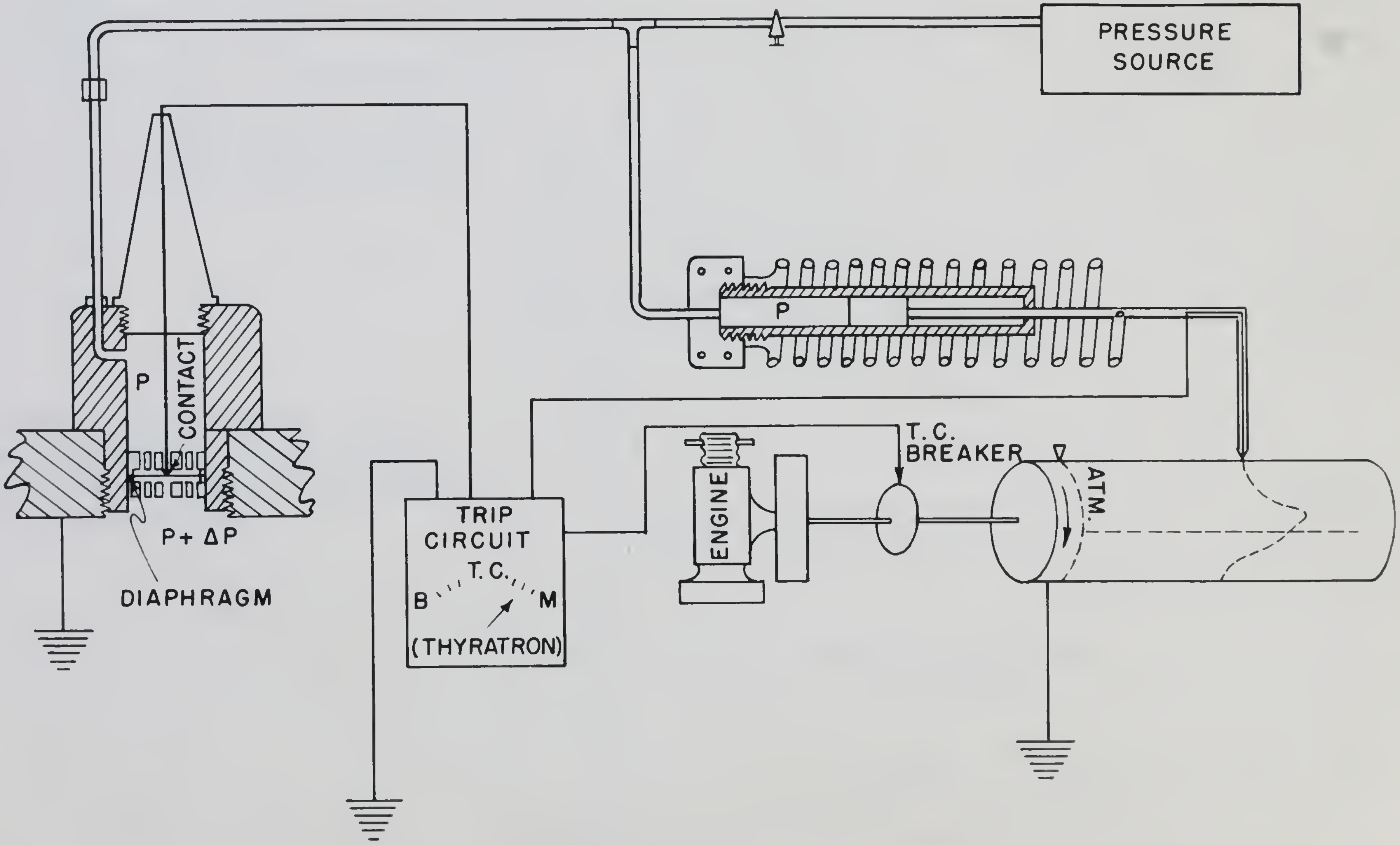

HIGH SPEED INDICATOR

M. I. T.

FIG. 4

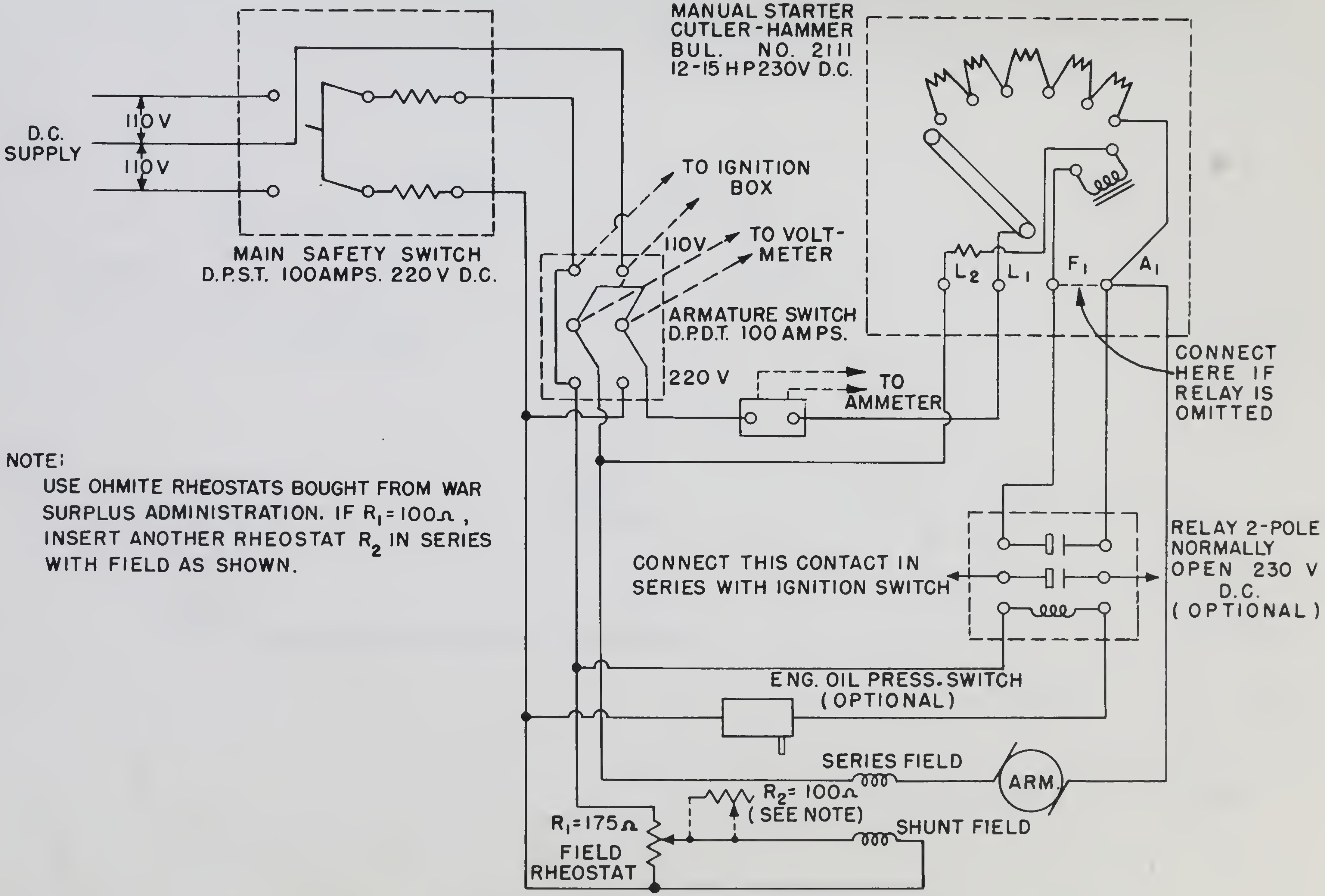

NOTE:

USE OHMITE RHEOSTATS BOUGHT FROM WAR SURPLUS ADMINISTRATION. IF $R_1 = 100\Omega$, INSERT ANOTHER RHEOSTAT R_2 IN SERIES WITH FIELD AS SHOWN.

WIRING DIAGRAM OF STAR DYNAMOMETER — CFR ENGINE SETUP

FIG. 5

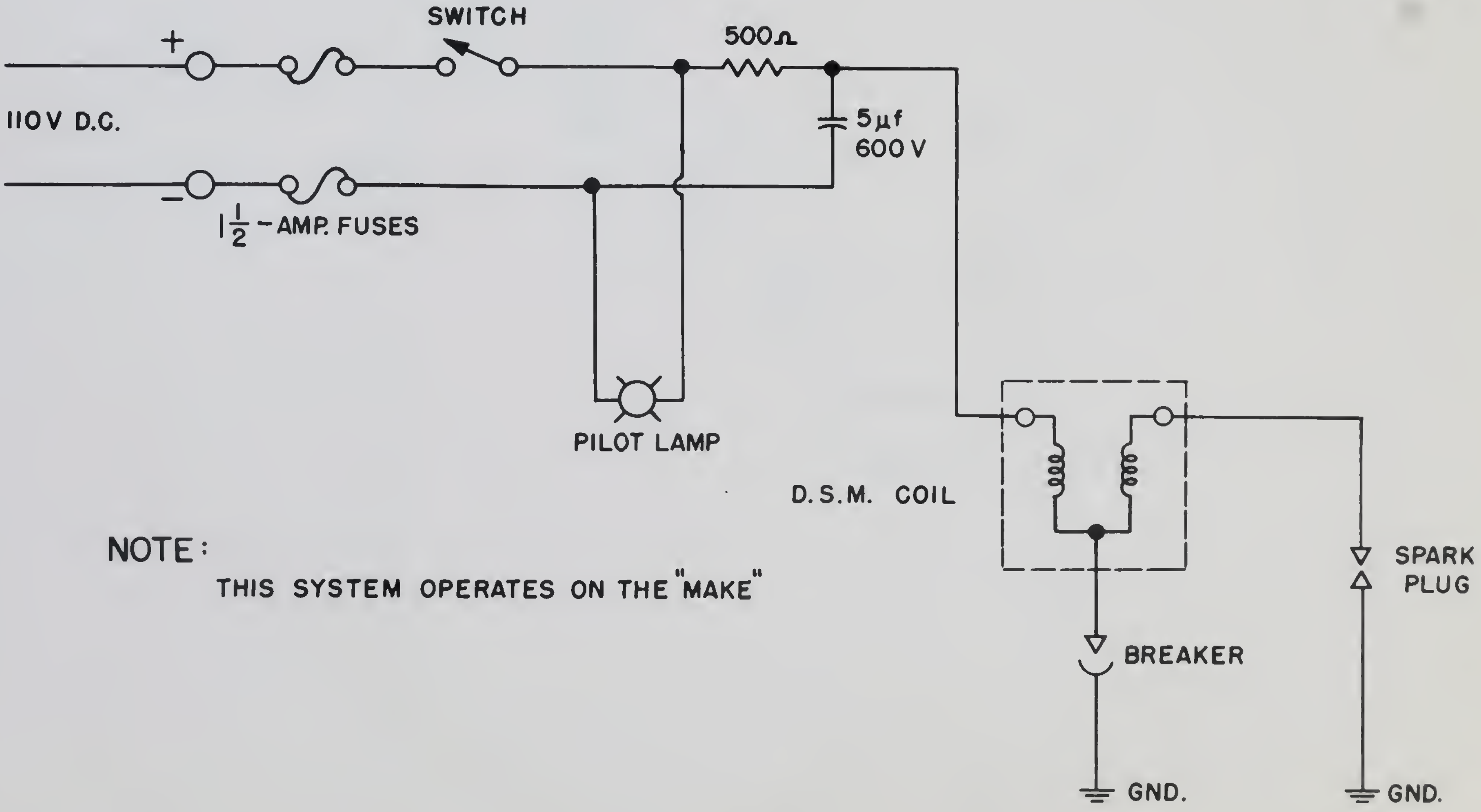

NOTE:

THIS SYSTEM OPERATES ON THE "MAKE"

WIRING DIAGRAM OF IGNITION SYSTEM

FIG. 6

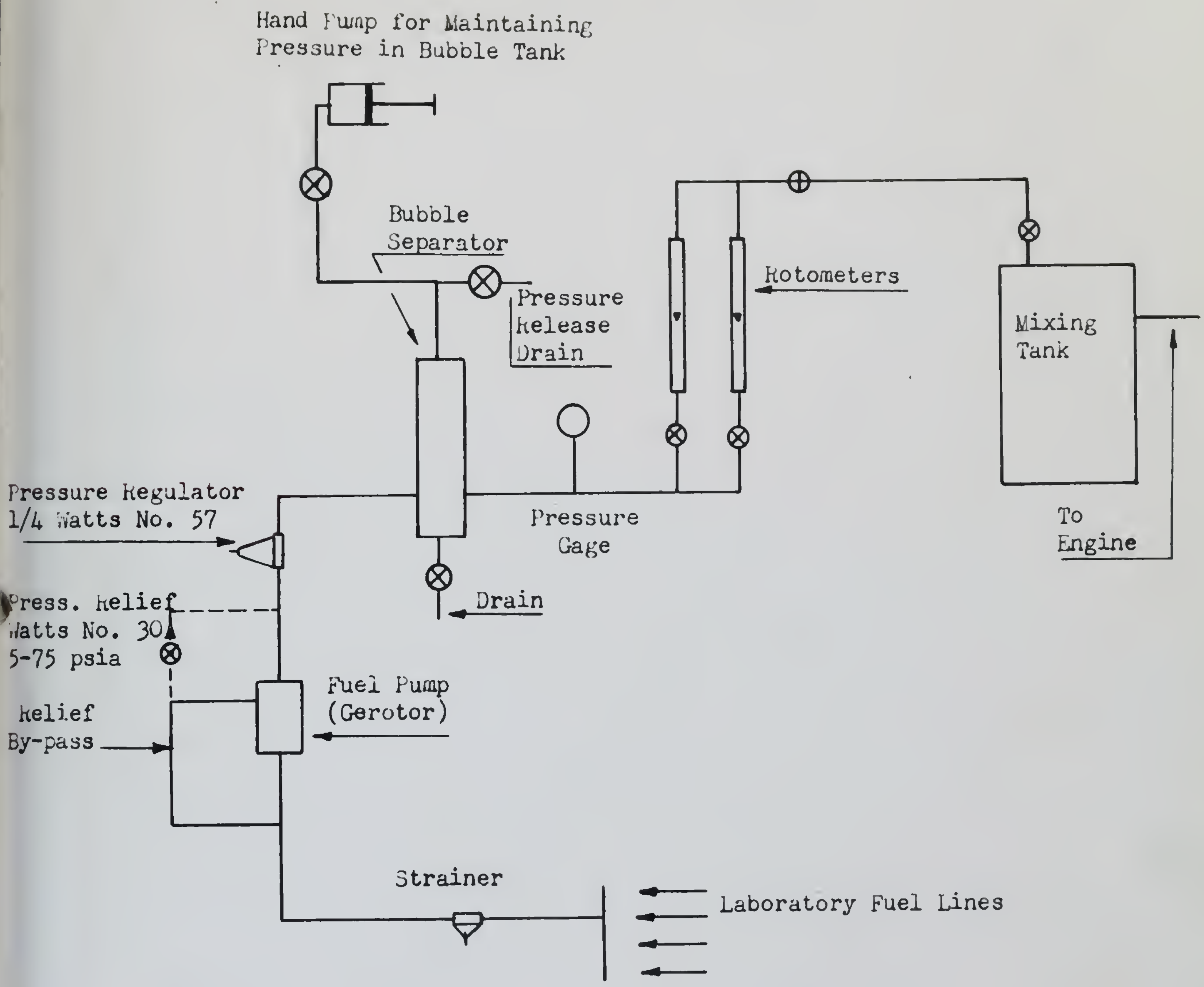

SCHEMATIC DIAGRAM OF FUEL SYSTEM

Fig.7

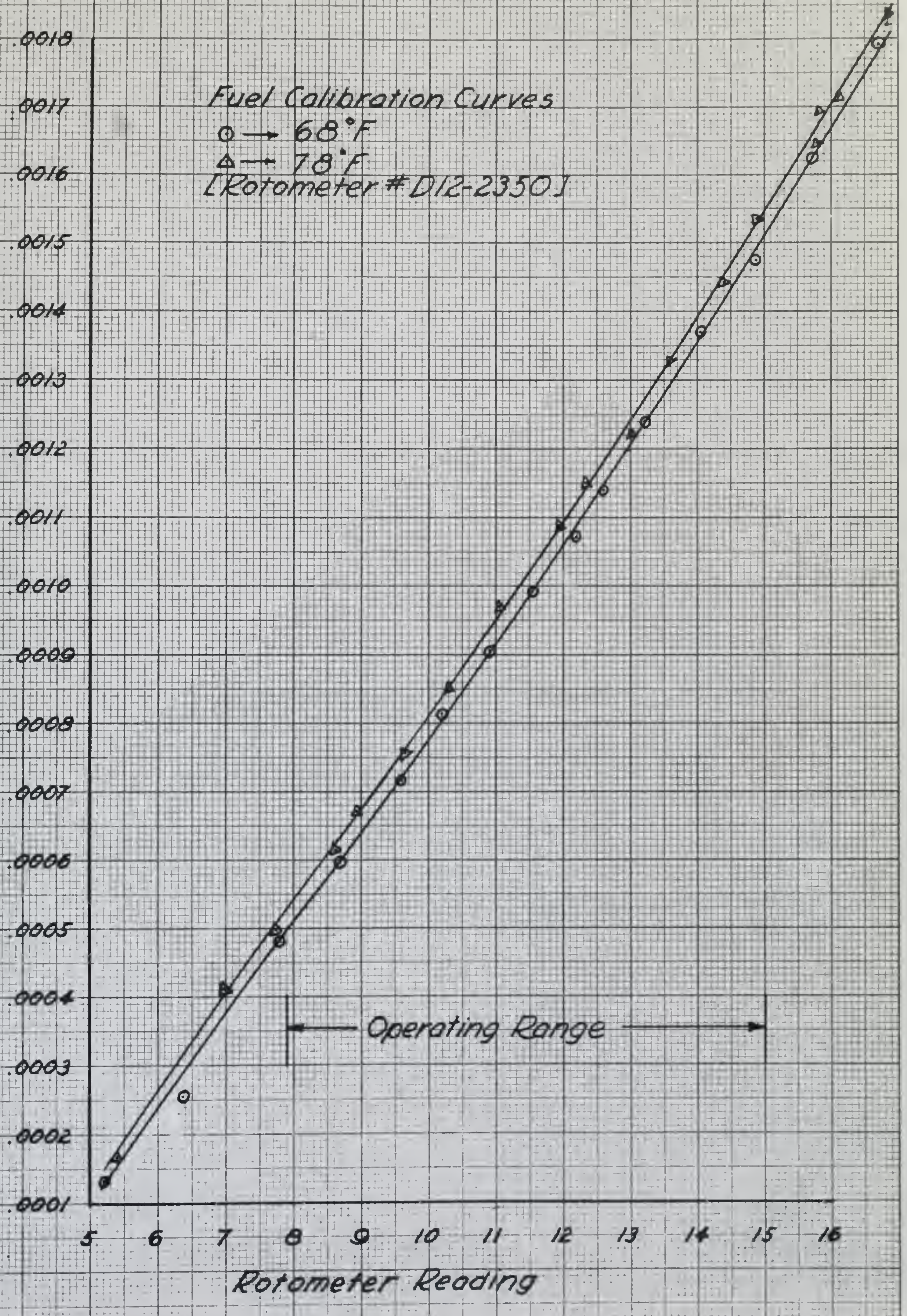
Fuel Calibration Curves
○ → 68°F
△ → 78°F
[Rotometer # D12-2350]
Operating Range
Fuel Flow - Pounds per Second
.0001
.0002
.0003
.0004
.0005
.0006
.0007
.0008
.0009
.0010
.0011
.0012
.0013
.0014
.0015
.0016
.0017
.0018
5
6
7
8
9
10
11
12
13
14
15
16
Rotometer Reading

Fig. 8

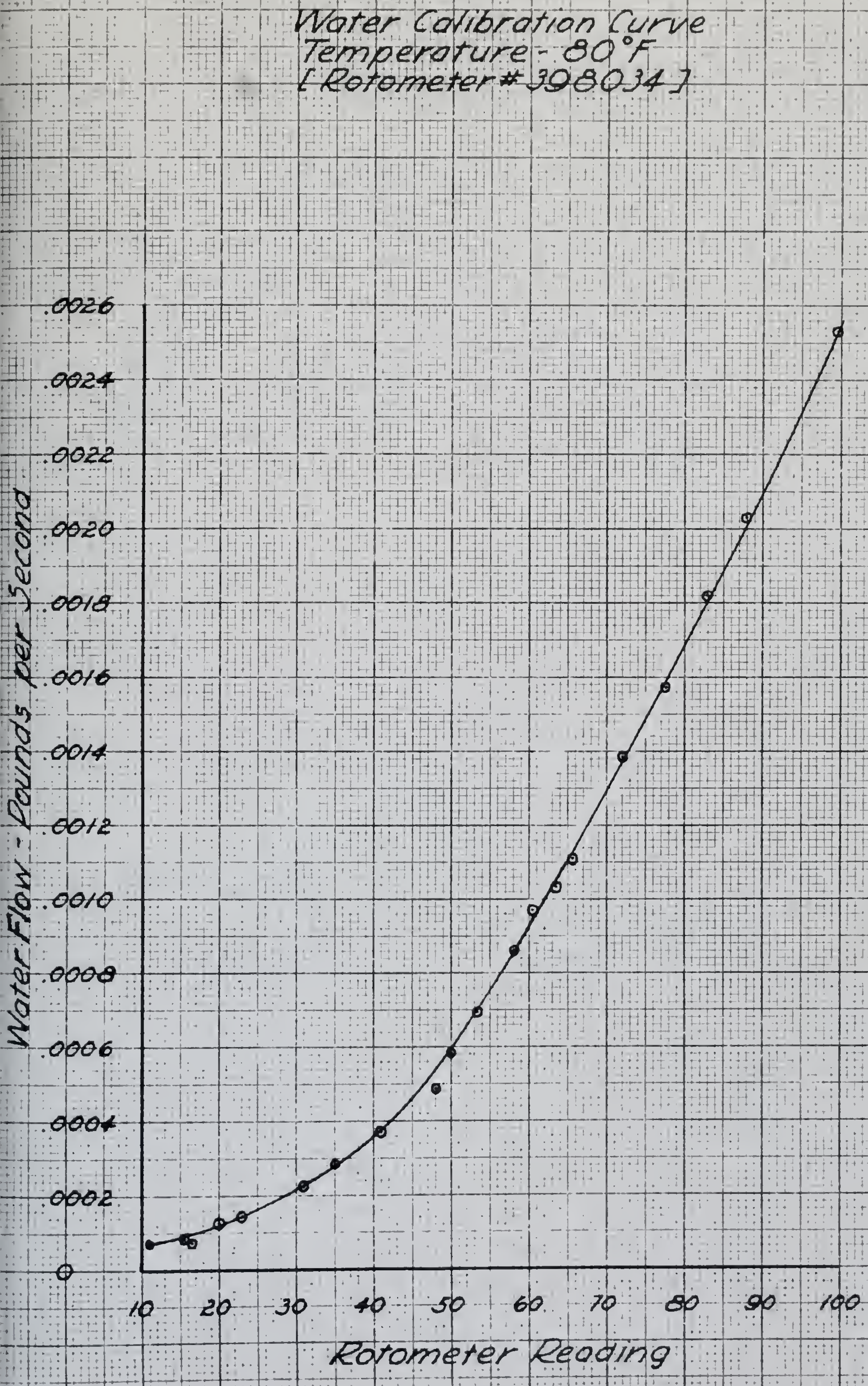

Water Calibration Curve
Temperature - 80°F
[Rotometer # 398034]
Water Flow - Pounds per Second
.0026
.0024
.0022
.0020
.0018
.0016
.0014
.0012
.0010
.0008
.0006
.0004
.0002
0
10
20
30
40
50
60
70
80
90
100
Rotometer Reading

Fig. 9

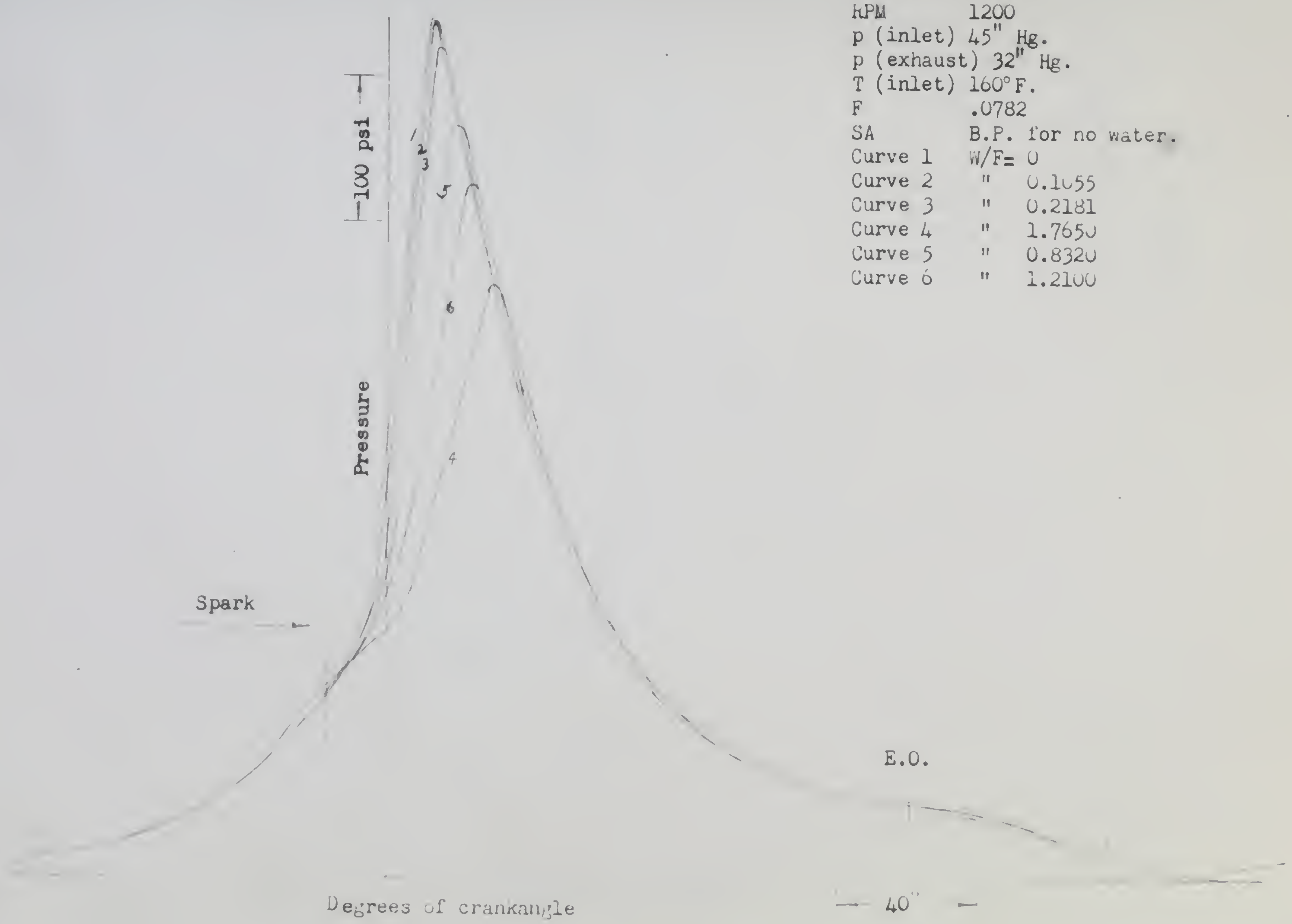
RPM 1200
p (inlet) 45" Hg.
p (exhaust) 32" Hg.
T (inlet) 160°F.
F .0782
SA B.P. for no water.
Curve 1 W/F= 0
Curve 2 " 0.1055
Curve 3 " 0.2181
Curve 4 " 1.7650
Curve 5 " 0.8320
Curve 6 " 1.2100
100 psi
Pressure
1
2
3
5
6
4
Spark
E.O.
Degrees of crankangle
40°

Fig. 10

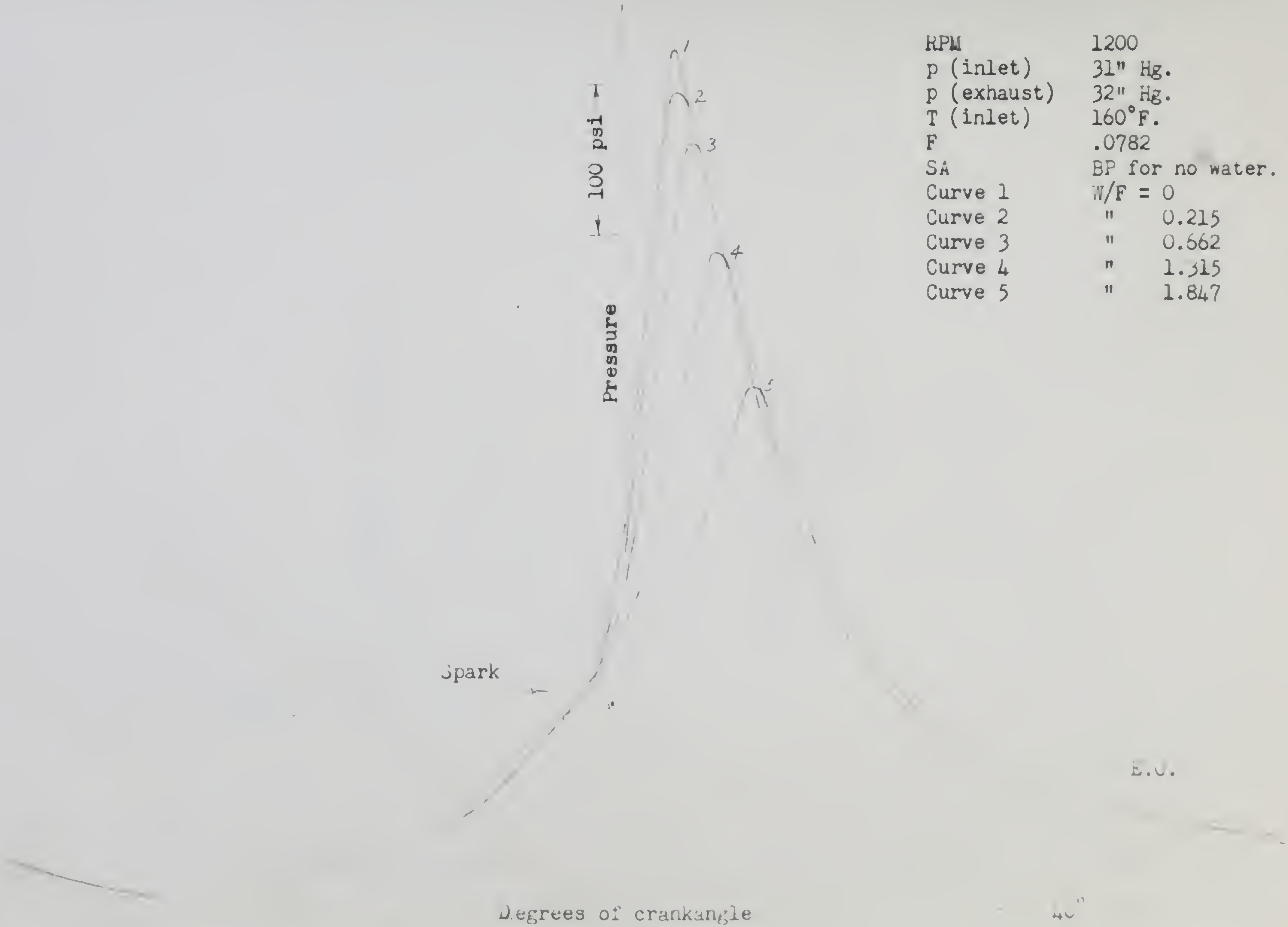
RPM 1200
p (inlet) 31" Hg.
p (exhaust) 32" Hg.
T (inlet) 160°F.
F .0782
SA BP for no water.
Curve 1 W/F = 0
Curve 2 " 0.215
Curve 3 " 0.662
Curve 4 " 1.315
Curve 5 " 1.847
100 psi
Pressure
1
2
3
4
5
Spark
E.O.
Degrees of crankangle
40°

Fig. 11

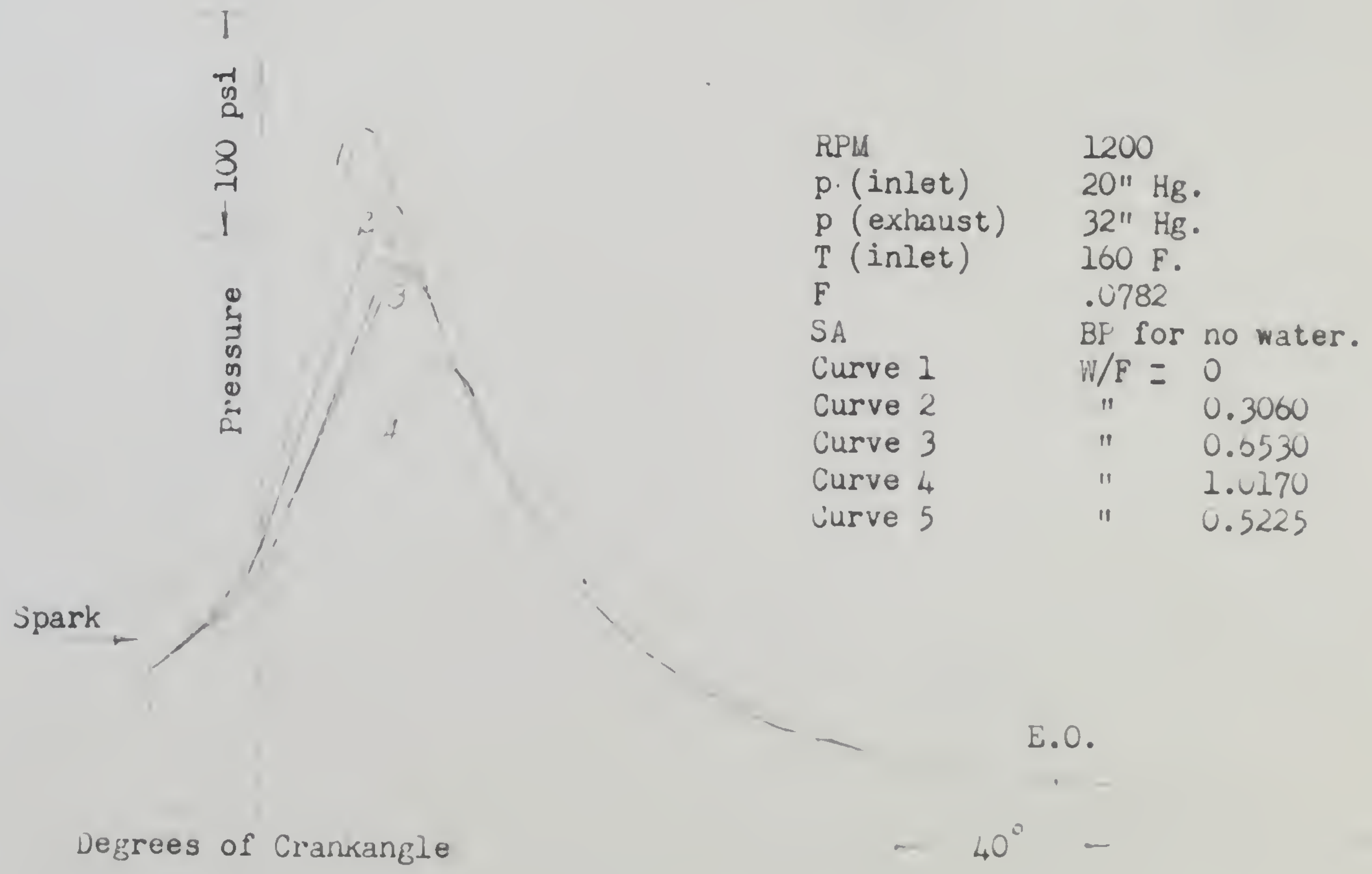

RPM	1200
p (inlet)	20" Hg.
p (exhaust)	32" Hg.
T (inlet)	160 F.
F	.0782
SA	BP for no water.
Curve 1	W/F = 0
Curve 2	" 0.3060
Curve 3	" 0.6530
Curve 4	" 1.0170
Curve 5	" 0.5225

Fig. 12

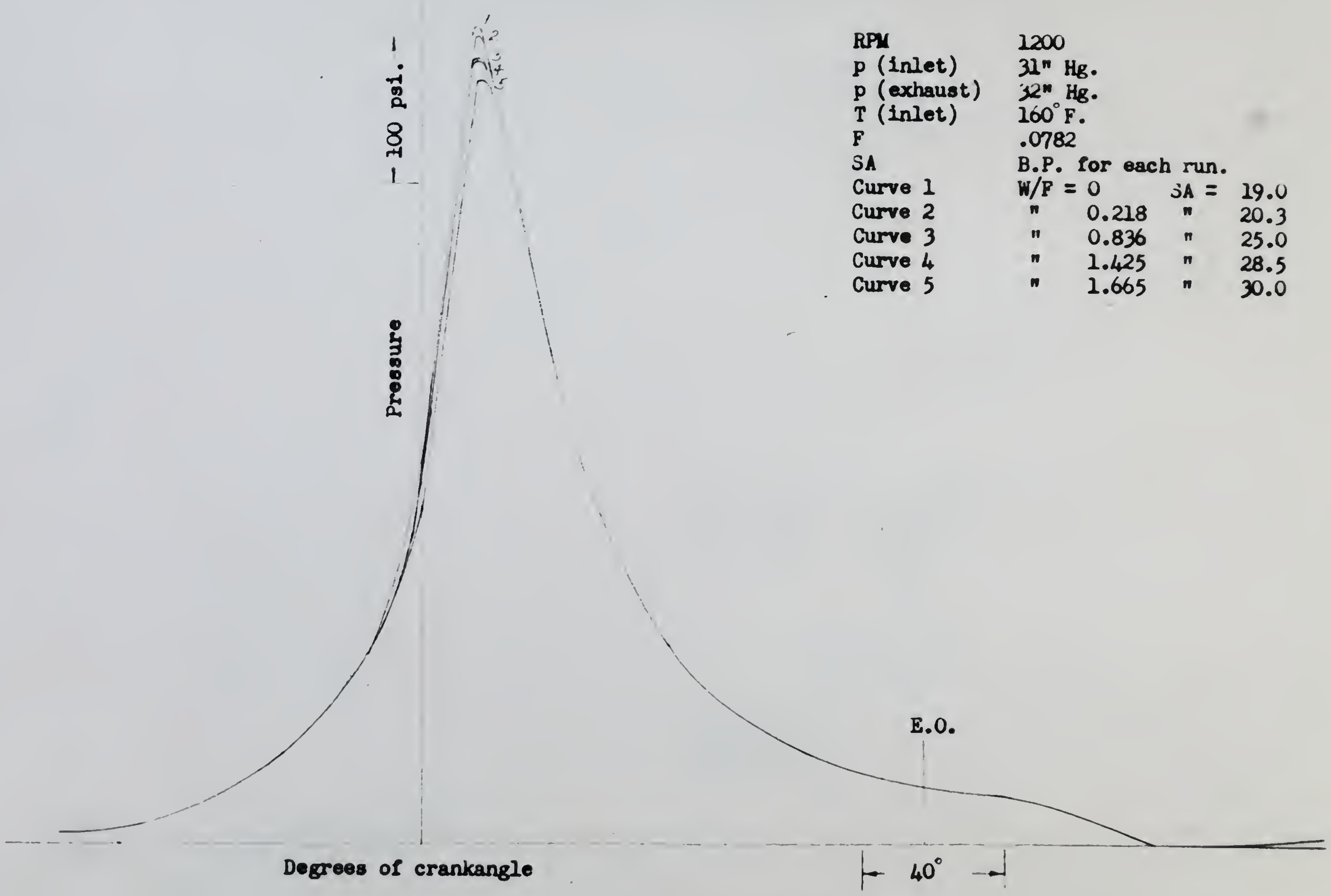

Fig. 13

RPM	1200		
p (inlet)	31" Hg.		
p (exhaust)	32" Hg.		
T (inlet)	160° F.		
F	.0782		
SA	B.P. for each run.		
Curve 1	W/F = 0	SA =	19.0
Curve 2	" 0.218	"	20.3
Curve 3	" 0.836	"	25.0
Curve 4	" 1.425	"	28.5
Curve 5	" 1.665	"	30.0

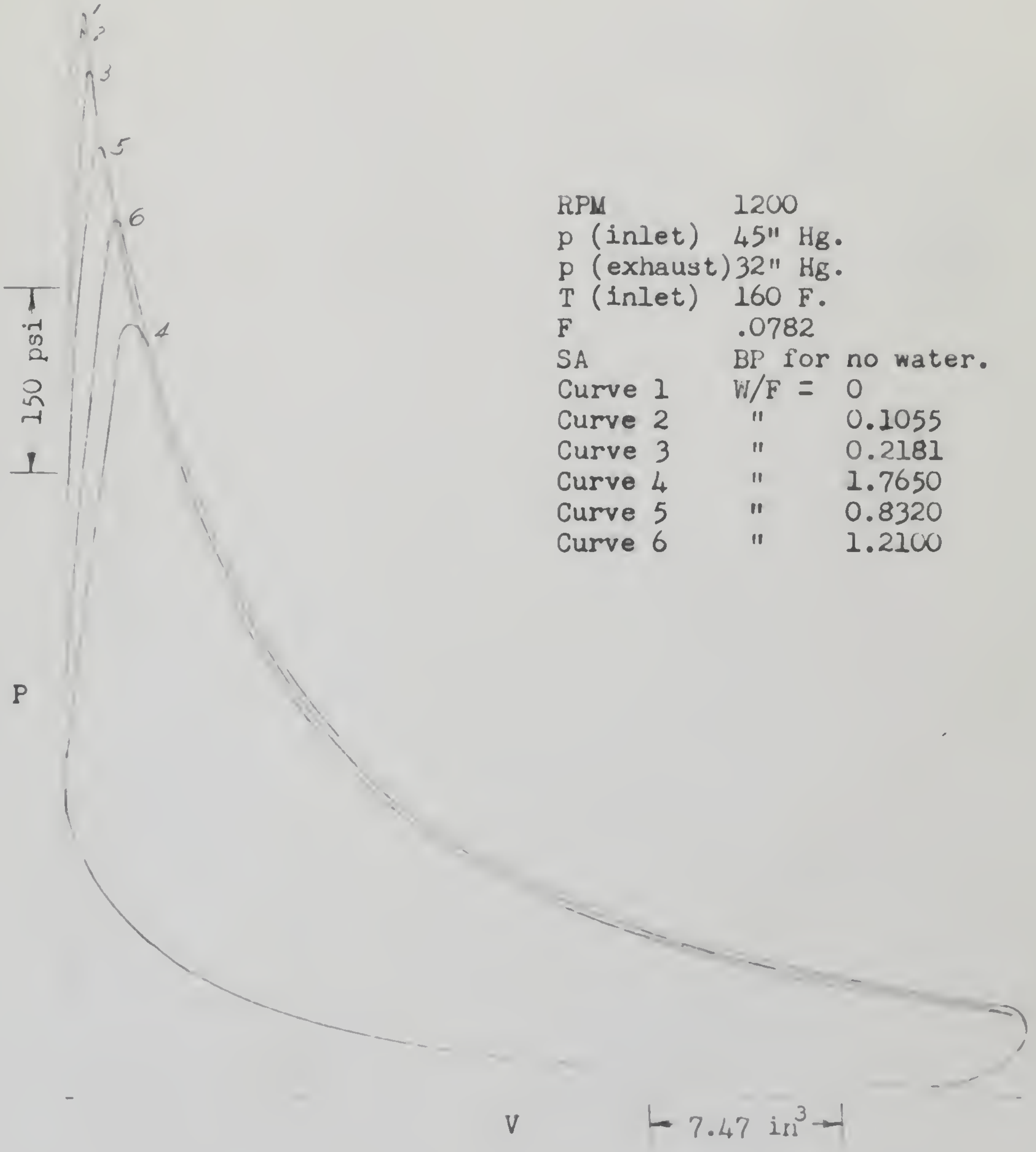

RPM	1200	
p (inlet)	45" Hg.	
p (exhaust)	32" Hg.	
T (inlet)	160 F.	
F	.0782	
SA	BP for no water.	
Curve 1	W/F =	0
Curve 2	"	0.1055
Curve 3	"	0.2181
Curve 4	"	1.7650
Curve 5	"	0.8320
Curve 6	"	1.2100

Fig. 14

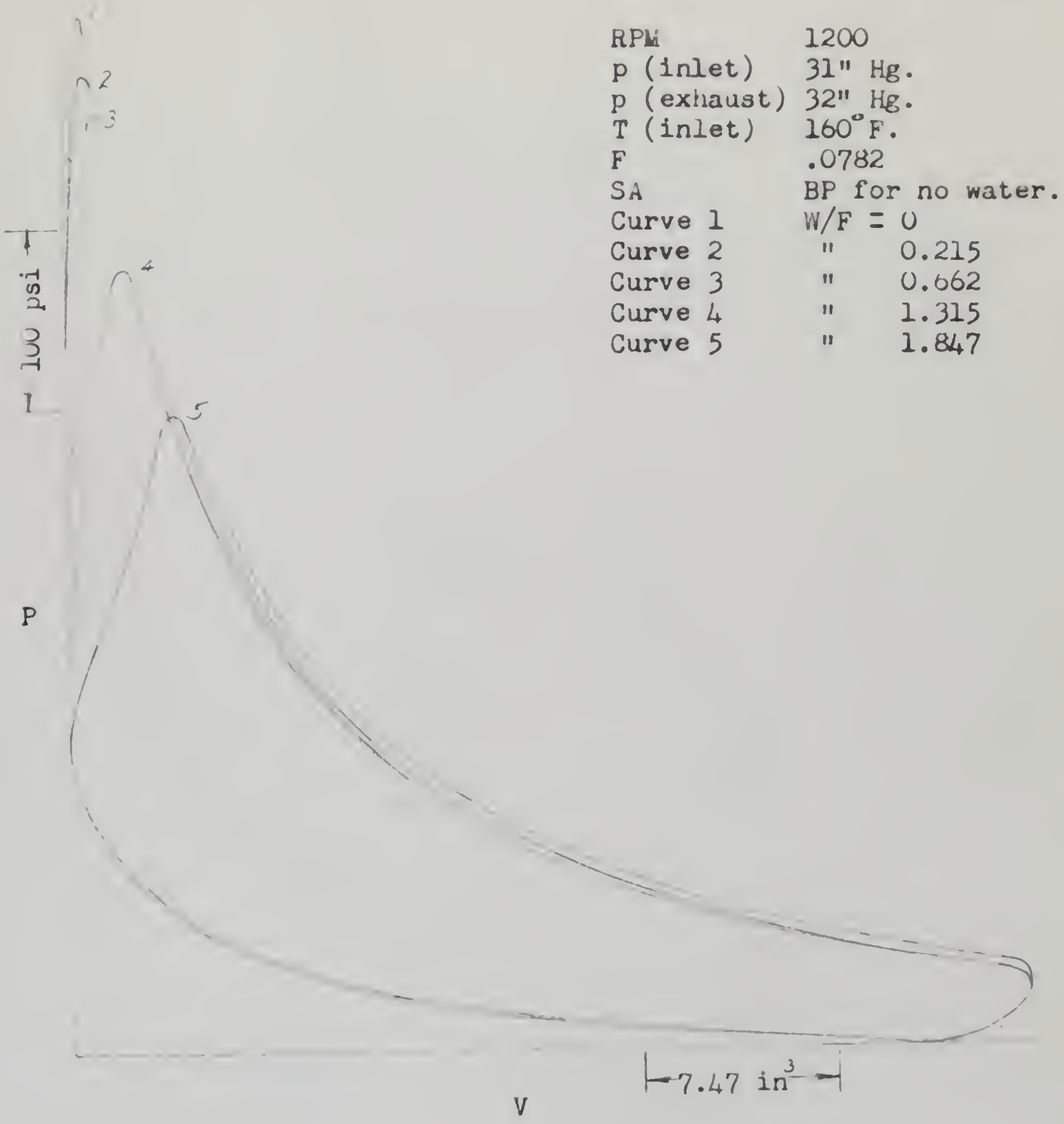

RPM	1200
p (inlet)	31" Hg.
p (exhaust)	32" Hg.
T (inlet)	160°F.
F	.0782
SA	BP for no water.
Curve 1	W/F = 0
Curve 2	" 0.215
Curve 3	" 0.662
Curve 4	" 1.315
Curve 5	" 1.847

Fig. 15

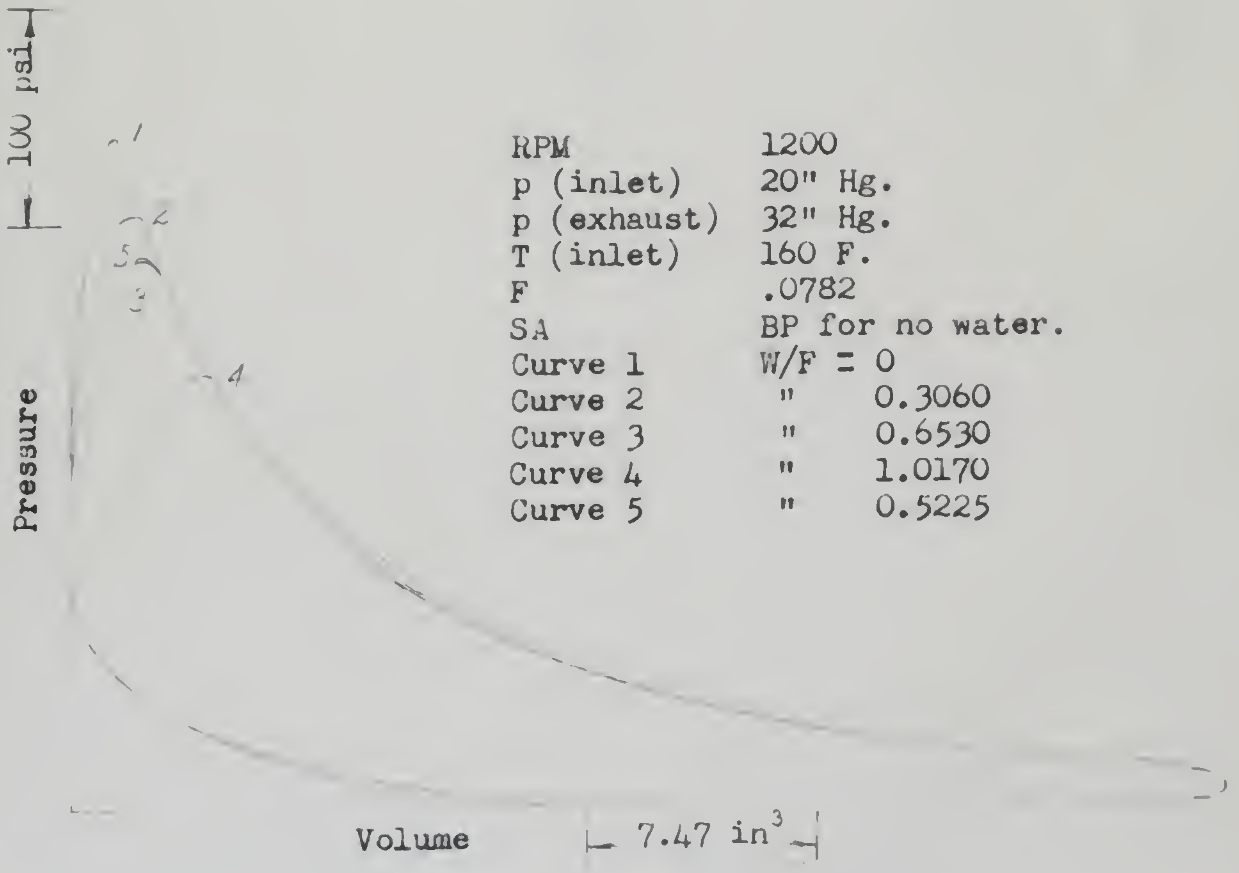
100 psi
Pressure
Volume
7.47 in³
1
2
5
3
4
RPM 1200
p (inlet) 20" Hg.
p (exhaust) 32" Hg.
T (inlet) 160 F.
F .0782
SA BP for no water.
Curve 1 W/F = 0
Curve 2 " 0.3060
Curve 3 " 0.6530
Curve 4 " 1.0170
Curve 5 " 0.5225

Fig. 16

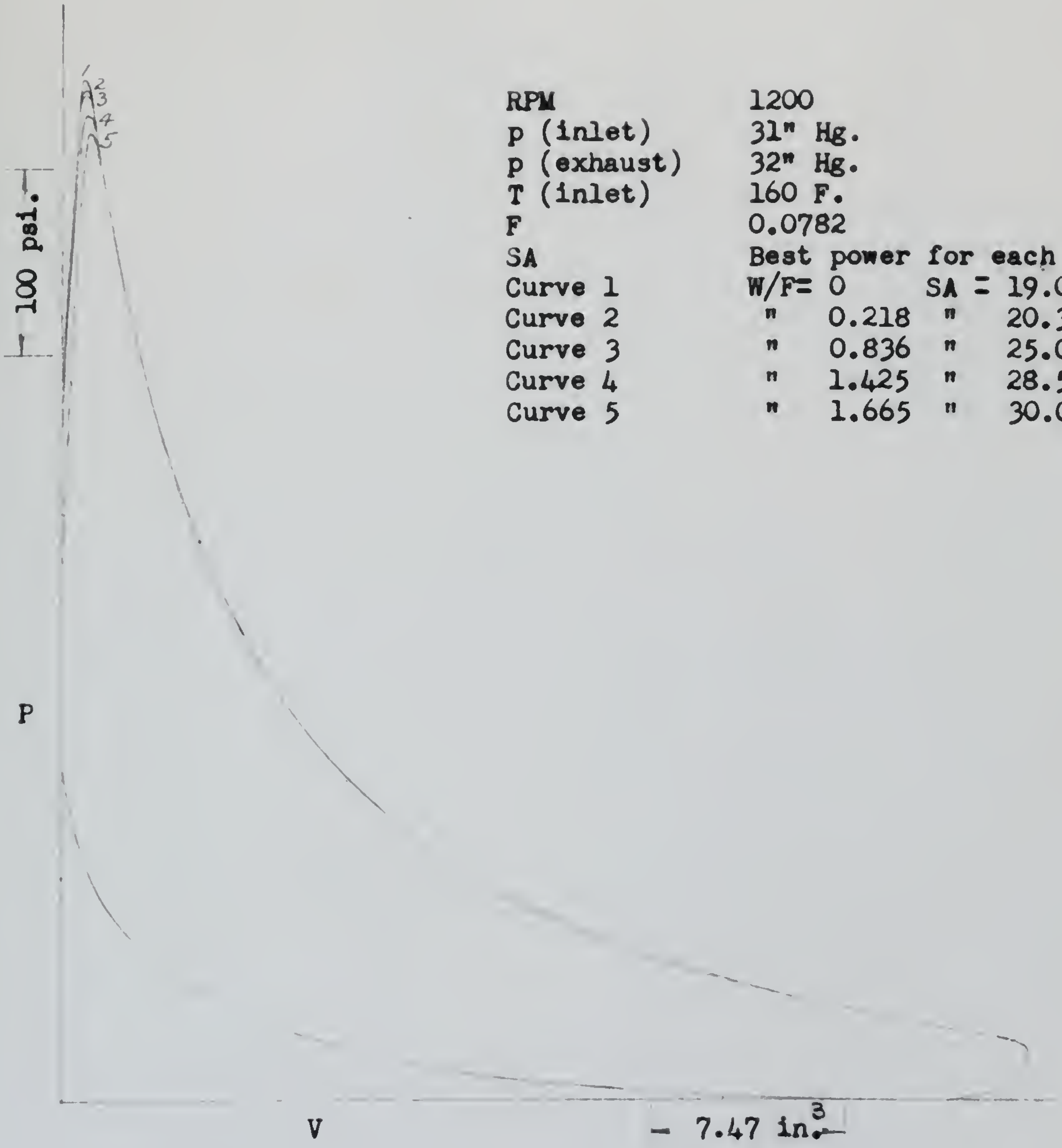

RPM 1200
p (inlet) 31" Hg.
p (exhaust) 32" Hg.
T (inlet) 160 F.
F 0.0782
SA Best power for each run.
Curve 1 W/F= 0 SA = 19.0
Curve 2 " 0.218 " 20.3
Curve 3 " 0.836 " 25.0
Curve 4 " 1.425 " 28.5
Curve 5 " 1.665 " 30.0

Fig. 17

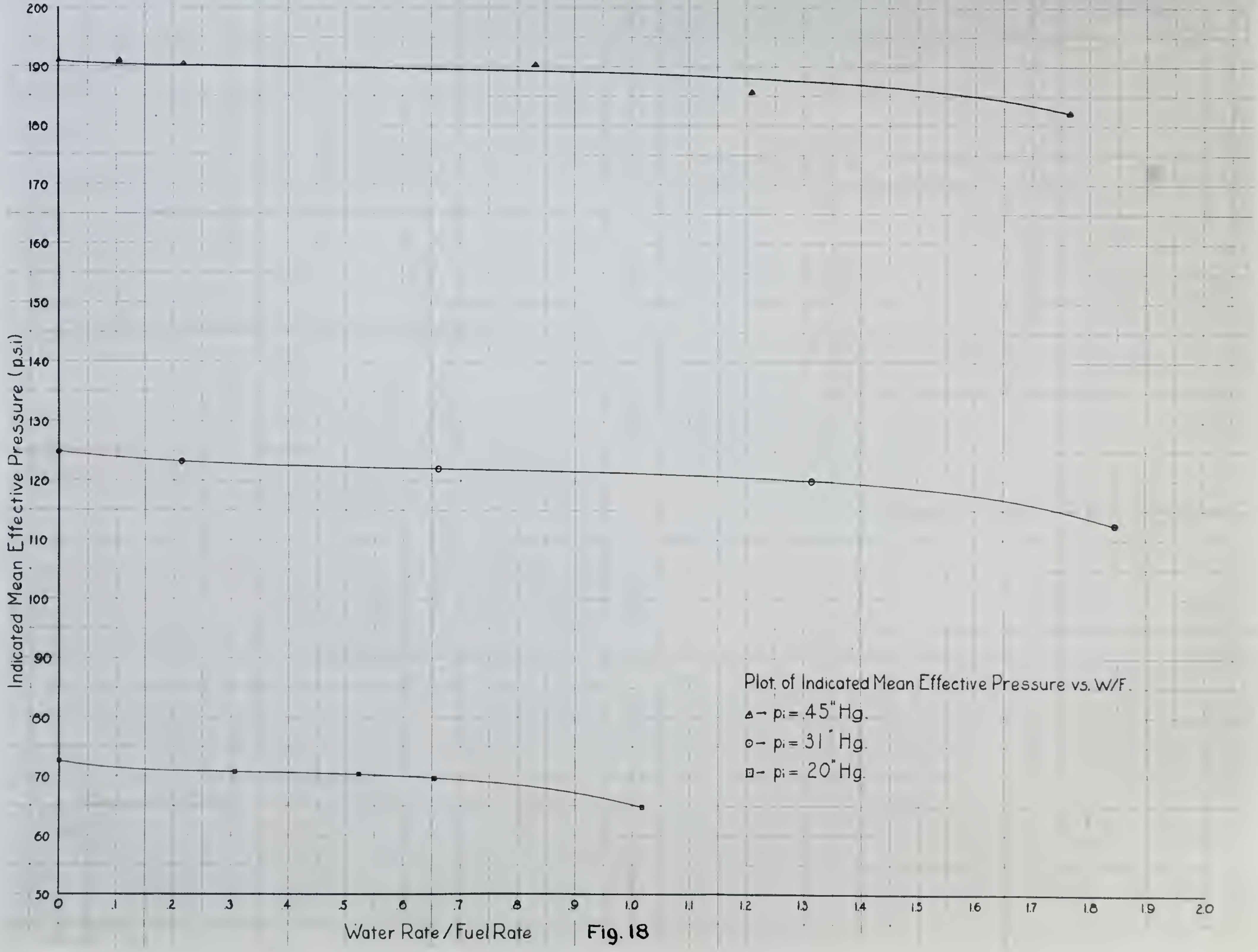
Plot. of Indicated Mean Effective Pressure vs. W/F.
▵ – pi = 45" Hg.
○ – pi = 31" Hg.
□ – pi = 20" Hg.
Indicated Mean Effective Pressure (p.s.i)
200
190
180
170
160
150
140
130
120
110
100
90
80
70
60
50
Water Rate / Fuel Rate
0
.1
.2
.3
.4
.5
.6
.7
.8
.9
1.0
1.1
1.2
1.3
1.4
1.5
1.6
1.7
1.8
1.9
2.0

Fig. 18

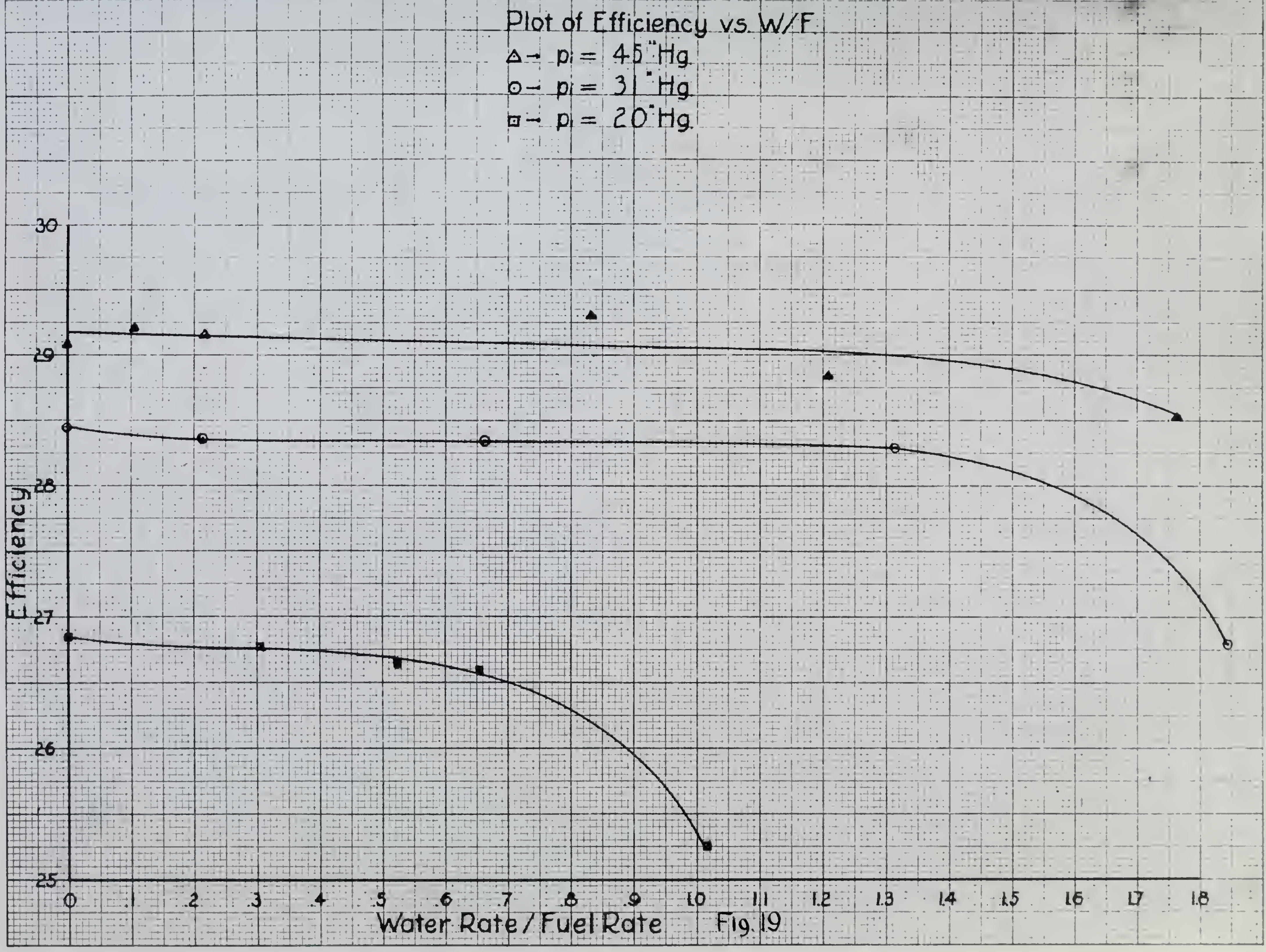
Plot of Efficiency vs. W/F
△→ pi = 45" Hg
⊙→ pi = 31" Hg
⊡→ pi = 20" Hg
Efficiency
30
29
28
27
26
25
0
.1
.2
.3
.4
.5
.6
.7
.8
.9
1.0
1.1
1.2
1.3
1.4
1.5
1.6
1.7
1.8
Water Rate / Fuel Rate

Fig. 19

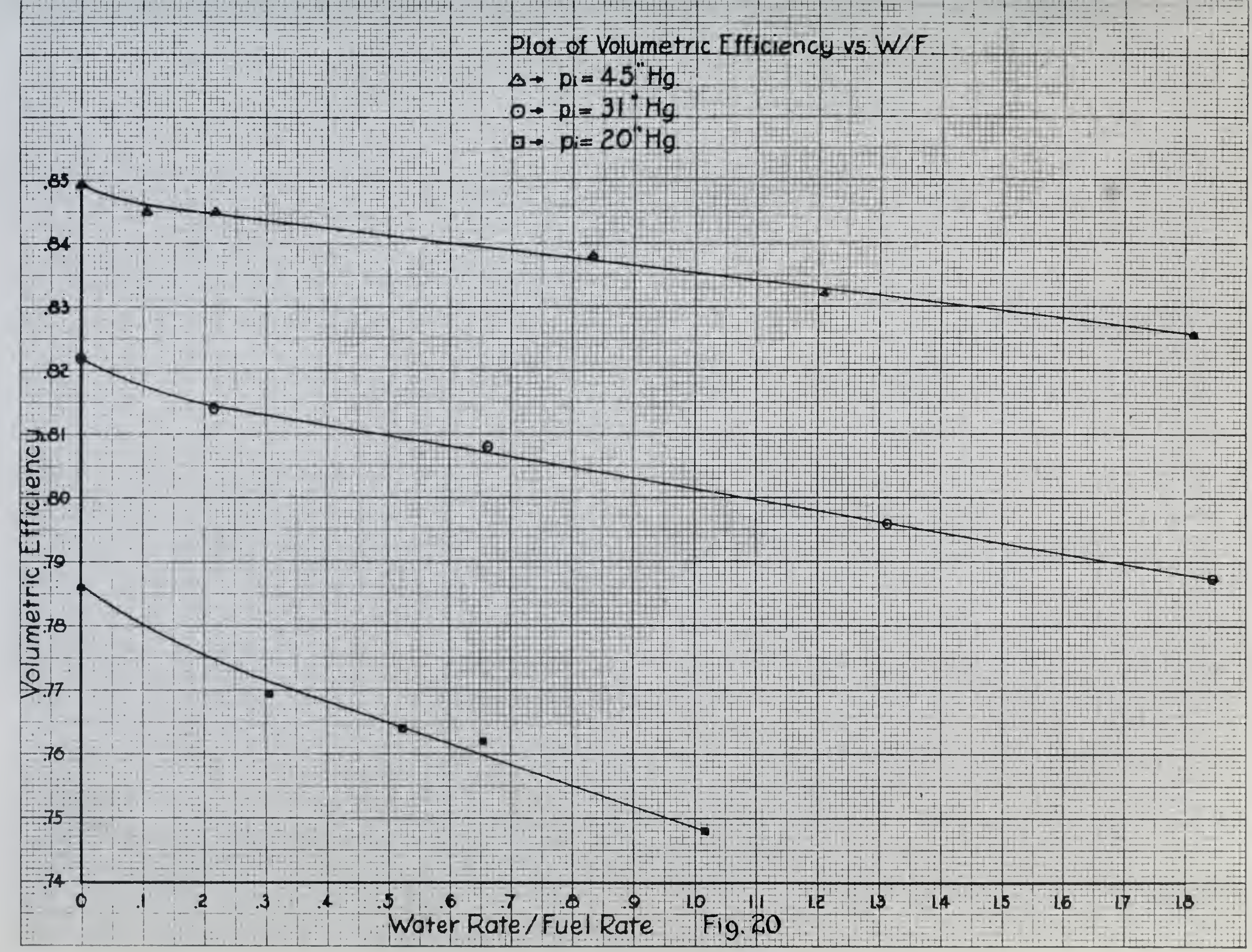
Plot of Volumetric Efficiency vs. W/F
△→ p_i = 45" Hg.
⊙→ p_i = 31" Hg.
⊡→ p_i = 20" Hg.
.85
.84
.83
.82
.81
.80
.79
.78
.77
.76
.75
.74
Volumetric Efficiency
0
.1
.2
.3
.4
.5
.6
.7
.8
.9
1.0
1.1
1.2
1.3
1.4
1.5
1.6
1.7
1.8
Water Rate / Fuel Rate

Fig. 20

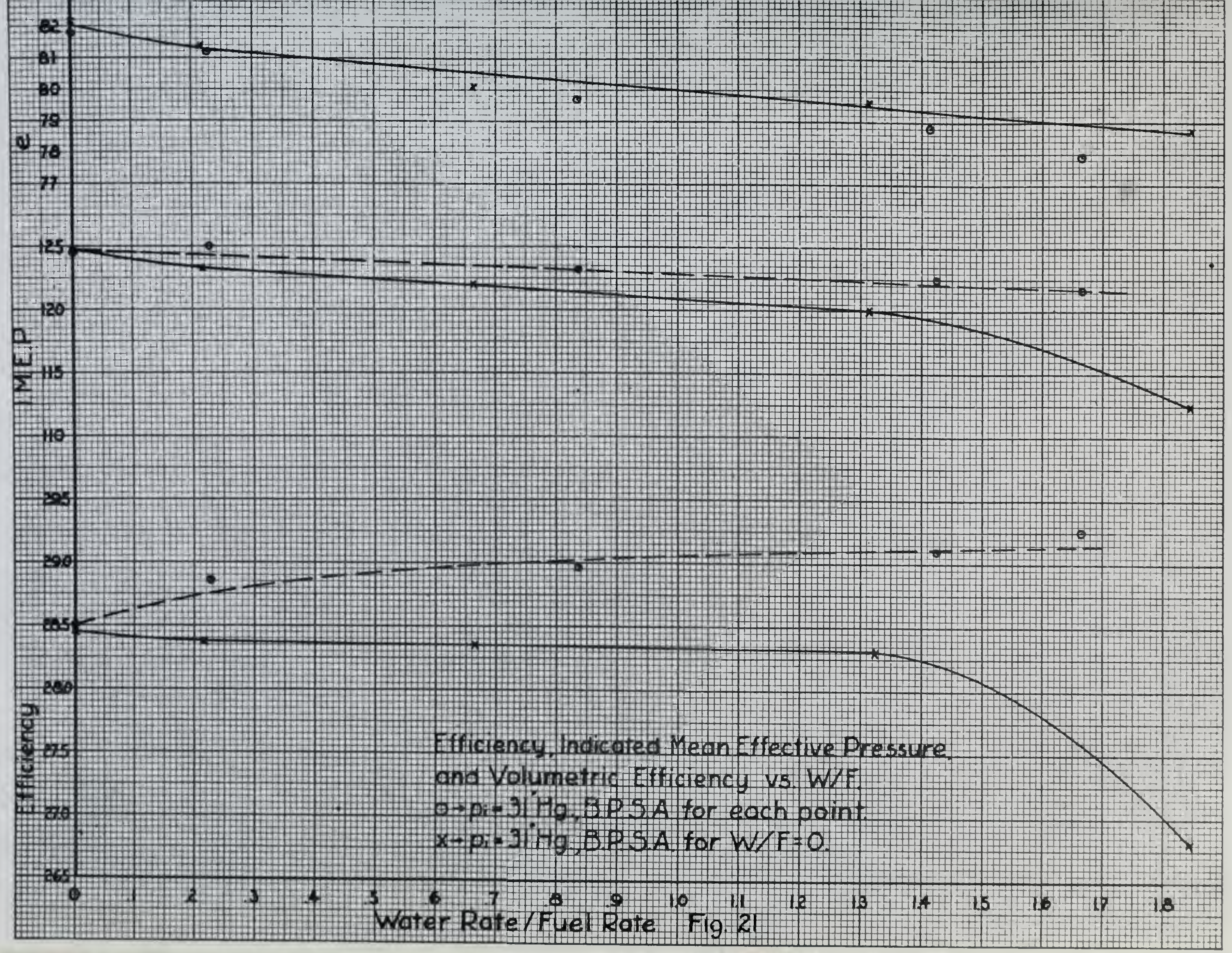

Efficiency, Indicated Mean Effective Pressure, and Volumetric Efficiency vs. W/F.
o→ p_i = 31" Hg., B.P.S.A. for each point.
x→ p_i = 31" Hg., B.P.S.A. for W/F = 0.

Fig. 21

Plot of Spark Advance vs. W/F
(B.P.S.A. for all points)

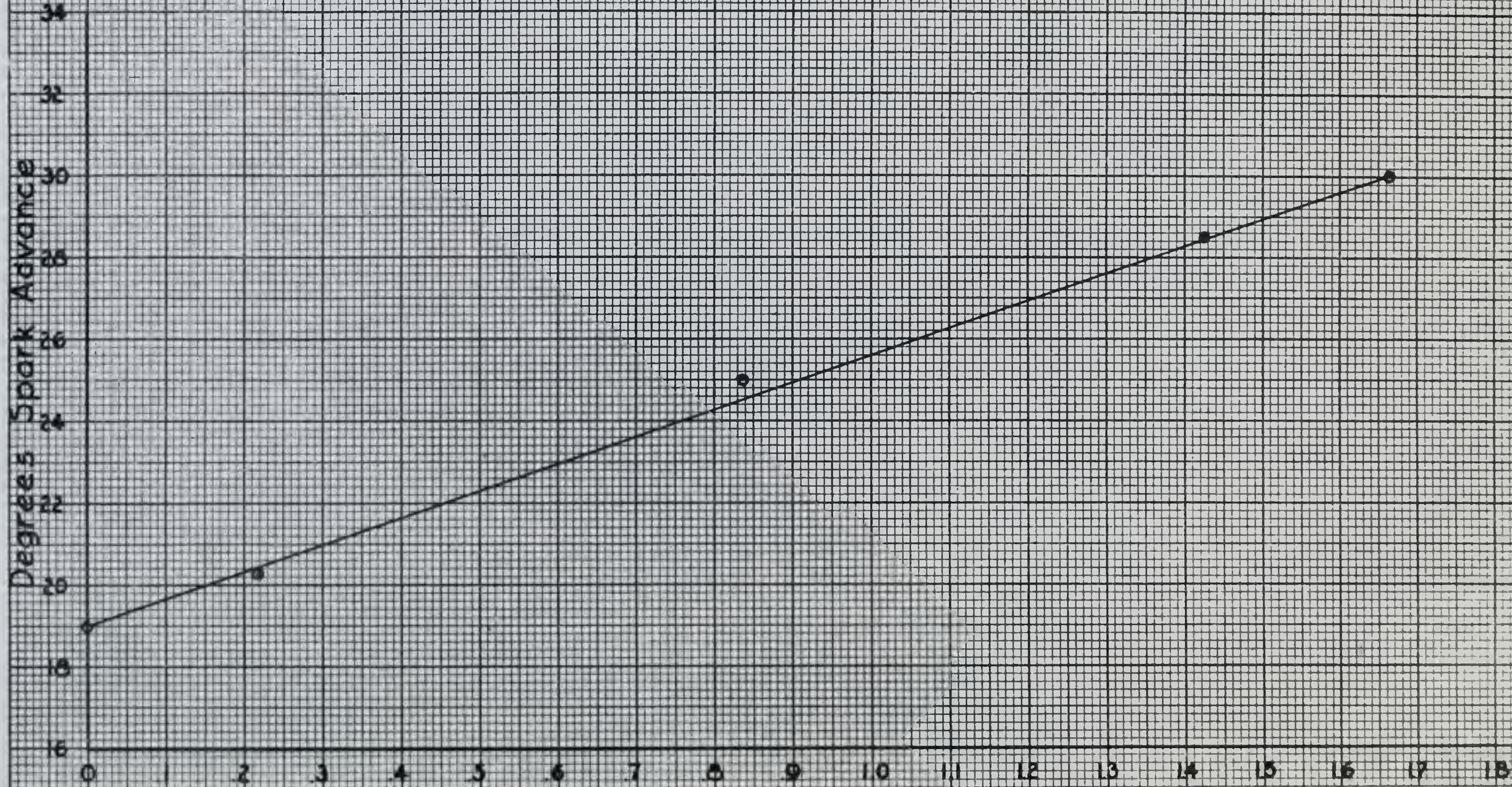

Fig 22

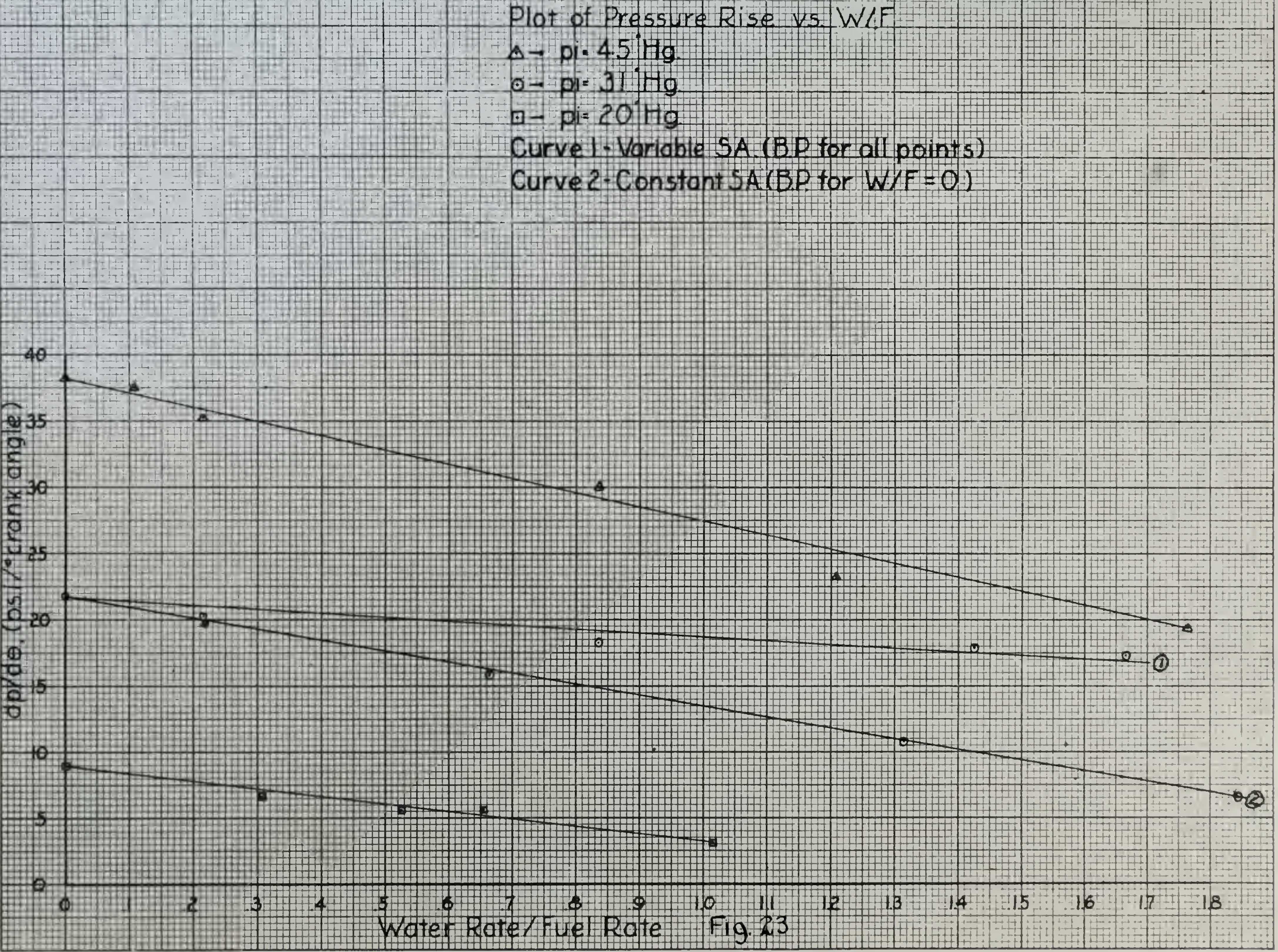

Plot of Pressure Rise vs. W/F

Fig. 23

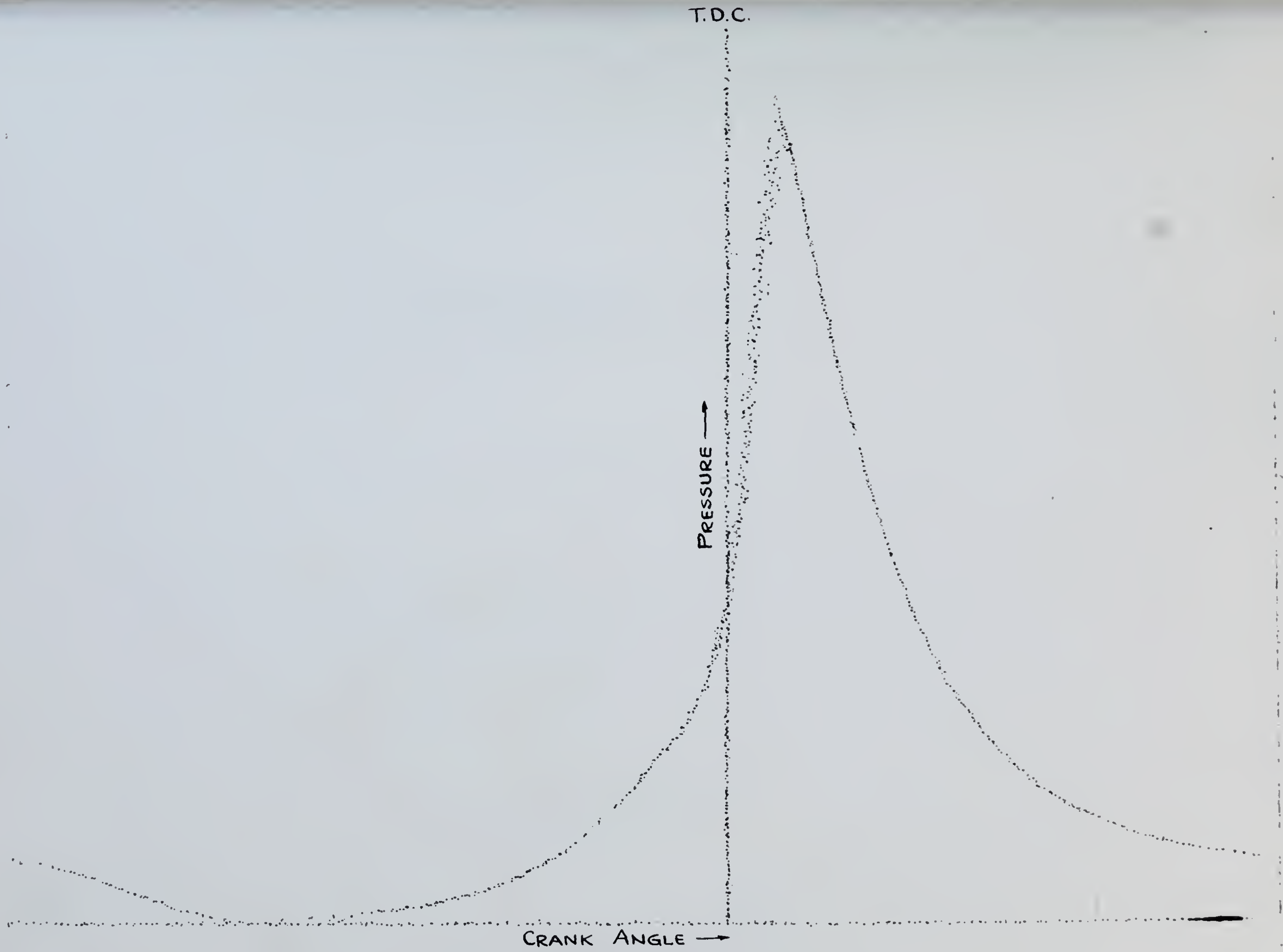

Sample Indicator Card (No Water Injected)

Fig. 24

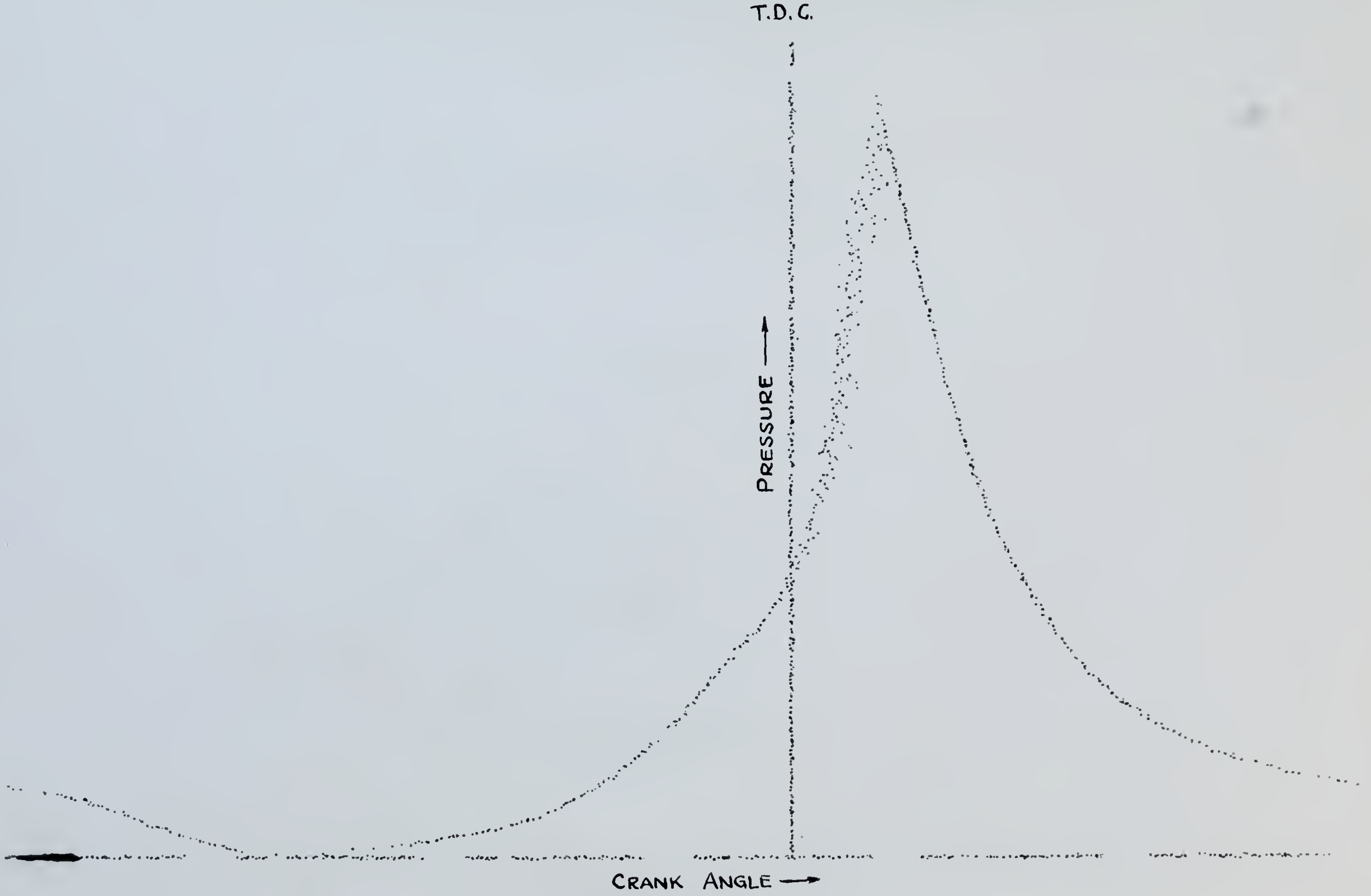

SAMPLE INDICATOR CARD (WITH WATER)

FIG. 25

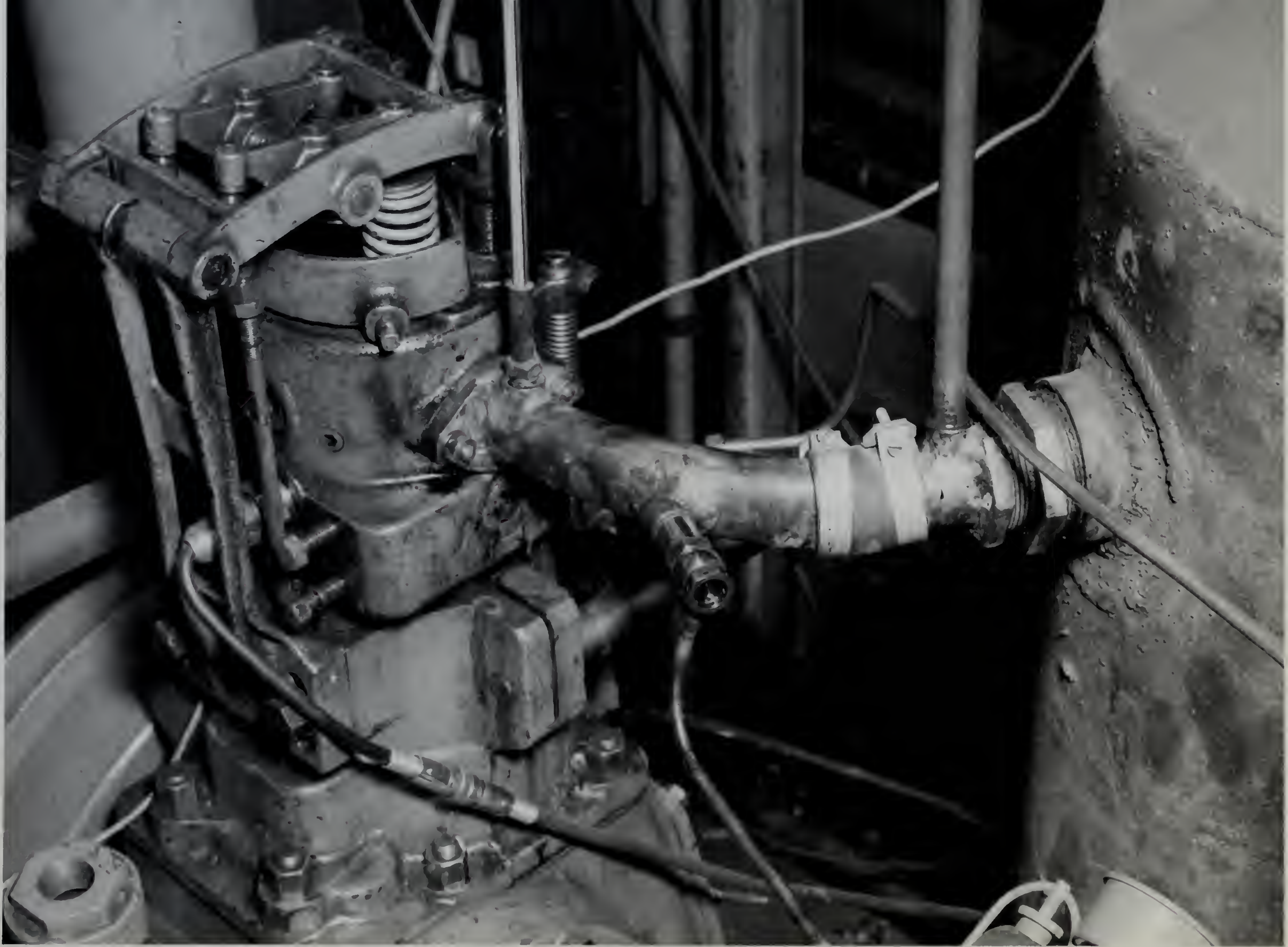

DETAIL- INLET MANIFOLD AND CYLINDER   FIG. 26

8092

Thesis W2

Wadsworth

The effect of water injection on the indicator card.

8092

Thesis W2

Wadsworth

The effect of water injection on the indicator card.

Library
U. S. Naval Postgraduate School
Monterey, California

thesW2
The effect of manifold water injection o
3 2768 001 92837 7
DUDLEY KNOX LIBRARY